Check for updates

# CO₂-assimilation, sequestration, and storage by urban woody species growing in parks and along streets in two climatic zones

Alessio Fini [a,*], Irene Vigevani [a,b,c], Denise Corsini [a,b], Piotr Węzyk [d,e], Katarzyna Bajorek-Zydroń [d], Osvaldo Failla [a], Edoardo Cagnolati [f], Lukasz Mielczarek [g], Sebastien Comin [a], Marco Gibin [a], Alice Pasquinelli [h], Francesco Ferrini [b,i], Paolo Viskanic [h]

[a] Department of Agricultural and Environmental Sciences—Production, Landscape, Agroenergy, University of Milan, Milan 20133, Italy
[b] Department of Agriculture, Food, Environment and Forestry, University of Florence, Florence 50144, Italy
[c] University School for Advanced Studies IUSS Pavia, Pavia 27100, Italy
[d] ProGea 4D sp. z o.o., ul. Pachońskiego 9, Kraków 31-223, Poland
[e] Department of Forest Resource Management, Faculty of Forestry, University of Agriculture in Kraków, Kraków 31-120, Poland
[f] Anthea S.r.l, Via della Lontra 30, Rimini 47923, Italy
[g] Zarząd Zieleni Miejskiej w Krakowie (ZZM), ul. Reymonta 20, Kraków 30-059, Poland
[h] R3 GIS S.r.l. NOI Techpark, D1, Via Ipazia 2, Bolzano 39100, Italy
[i] National Biodiversity Future Center, Italy

## HIGHLIGHTS

- The reduction of atmospheric CO₂ by 15 species growing in cities was evaluated.
- CO₂-assimilation and storage were measured using infra-red gas analyser and TLS-LiDAR.
- Photosynthetic rate and LAI affect species effectiveness for CO₂ uptake.
- The amount of assimilated CO₂ which gets sequestered decreases with tree age.
- Management associated to park and street trees can affect CO₂-removal.

## GRAPHICAL ABSTRACT
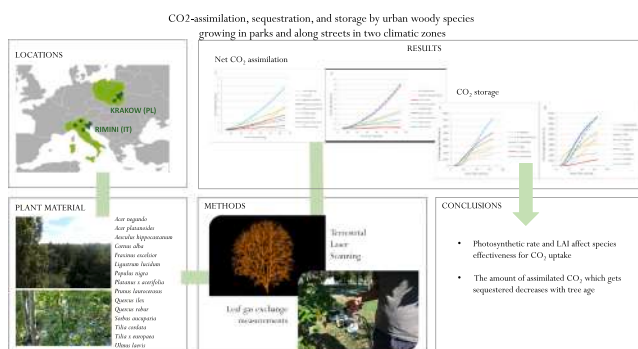


## ARTICLE INFO

## ABSTRACT

Using two cities, Rimini (Italy, Cfa climate) and Krakow (Poland, Cfb), as living laboratories, this research aimed at measuring in situ the capacity of 15 woody species to assimilate, sequester, and store CO₂. About 1712 trees of the selected species were identified in parks or along streets of the two cities, and their age, DBH, height, and crown radius were measured. The volume of trunk and branches was measured using a terrestrial LiDAR. The true Leaf Area Index was calculated by correcting transmittance measurements conducted using a plant-canopy-analyser for leaf angle distribution, woody area index, and clumping. Dendrometric traits were fitted using age or DBH as independent variable to obtain site- and species-specific allometric equations. Instantaneous and daily net CO₂-assimilation per unit leaf area was measured using an infra-red gas-analyser on full-sun and shaded

leaves and upscaled to the unit crown-projection area and to the whole tree using both a big-leaf and a multilayer approach. Results showed that species differed for net $CO_2$-assimilation per unit leaf area, leaf area index, and for the contribution of shaded leaves to overall canopy carbon gain, which yielded significant differences among species in net $CO_2$-assimilation per unit crown-projection-area ($A_{cpaML(d)}$). $A_{cpaML(d)}$ was underestimated by 6–30 % when calculated using the big-leaf, compared to the multilayer model. While maximizing $A_{cpaML(d)}$ can maximize $CO_2$-assimilation for a given canopy cover, species which matched high $A_{cpaML(d)}$ and massive canopy spread, such as mature *Platanus x acerifolia* and *Quercus robur*, provided higher $CO_2$-assimilation ($A_{tree}$) at the individual tree scale. Land use (park or street), did not consistently affect $CO_2$-assimilation per unit leaf or crown-projection area, although $A_{tree}$ can decline in response to specific management practices (e.g. heavy pruning). $CO_2$-storage and sequestration, in general, showed a similar pattern as $A_{tree}$, although the ratio between $CO_2$-sequestration and $CO_2$-assimilation decreased at increasing DBH.

## 1. Introduction

Atmospheric $CO_2$ concentration has increased significantly due to anthropogenic sources, resulting in $CO_2$ being the single most important driver of anthropogenic climate change with urban areas as "hotspots" for its emission (Grimm et al., 2008). Therefore, information on the contribution from the different $CO_2$ sources and sinks in the urban environment is needed at fine spatial resolution to help develop local greening programs to mitigate and to adapt to climate change effects. Based on this municipalities around the world have adopted policies promoting massive tree-planting and the preservation of urban green spaces, but since cities differ in many aspects, the amount of carbon stored in trees differs strongly between them (Nowak et al., 2013). Studies are needed to complement previous findings with additional carbon storage values to result in realistic estimates and improve accuracy of global carbon storage models.

No method currently exists that can directly evaluate the $CO_2$-uptake by urban greenery and most widely used approaches rely on indirect estimates and are prone to uncertainties (Velasco et al., 2016). $CO_2$-uptake has frequently been quantified as C- or $CO_2$-storage (i.e. the amount of atmospheric carbon or $CO_2$ trapped as organic carbon in the wood of trunk, primary branches and main roots) and as C- or $CO_2$-sequestration (i.e. the change in storage over 1 year) (Nowak and Crane, 2002). $CO_2$-storage and sequestration are in most cases estimated from plant dry biomass or volume (Picard et al., 2012). Because of technical challenges in direct measurement of biomass or volume at urban sites, they are often indirectly estimated using allometric equations (Jo and McPherson, 1995). The widespread adoption of equations from forest trees, due to limited information about allometry of open-grown trees, is a major source of uncertainty associated to allometric equations (Yoon et al., 2013). Such uncertainty is further enhanced by the high heterogeneity of urban settings, where trees growing in park and gardens may experience different growing conditions and management practices than street trees.

Recent advances in Terrestrial Laser Scanning (TLS LiDAR) enabled the acquisition of a dense 3D point clouds and the accompaning development of tree segmentation methods allowed the modelling of trunk and main branches. This provided the opportunity of large-scale data collection for the development of specific algorithms (like TreeQSM) for 3D quantitative structure models opening new possibilities to reconstruct tree architecture and calculate tree volume (Raumonen et al., 2013; Fan et al., 2020).

$CO_2$-storage and sequestration, however, may not fully capture the contribution of vegetation to $CO_2$-uptake. When $CO_2$-sequestration was compared to photosynthetic $CO_2$-assimilation (i.e. gross primary productivity minus autotrophic respiration) estimated by Eddy Covariance, the former method underestimated net primary productivity by 20–60 % (Velasco et al., 2016). To include photosynthetic traits in the estimation of $CO_2$ uptake by urban vegetation, empiric and process-based models were recently proposed (Weissert et al., 2017; Rötzer et al., 2019; Fares et al., 2020). Most process-based models use biochemical models of photosynthesis (Farquhar et al., 1980) for the real-time estimation of $CO_2$-assimilation based on environmental parameters, but their use is constrained by labour-intensive characterization of photosynthetic traits (e.g. apparent maximum carboxylation rate, $V_{cmax,Ci}$) which makes challenging to obtain representative estimates for the different species, climatic zones, and urban land-uses. Proxying $V_{cmax,Ci}$ with the indirect estimation from leaf-nitrogen (De Pury and Farquhar, 1997) or literature data may lead to inaccuracies because $V_{cmax,Ci}$ is subjected to even greater short-term dynamic changes than $CO_2$-assimilation itself when mesophyll limitations constrain photosynthesis during stress (Fini et al., 2014; Brunetti et al., 2019). More data about $CO_2$-assimilation by different types of urban vegetation are needed for a proper validation of process-based models, but direct measurements of $CO_2$-assimilation have seldom been conducted in situ at the city scale (Weissert et al., 2017). Thus, there is still uncertainty about the major photosynthetic traits of widely used urban species, as well as about how they are affected by major conflicts with the grey infrastructure (e.g. soil sealing) (Savi et al., 2015; Fini et al., 2022). For example, the mechanisms adopted by the different species to cope with drought (e.g. isohydric/anisohydric) are debated or unknown for several widely-used urban species and cultivars, and few evidences exist about how such mechanisms may affect ecosystem services provisioning (Kannenberg et al., 2022).

Upscaling $CO_2$-assimilation per unit leaf area to the canopy has long been debated in the framework of the dichotomy between the "incorrect but useful" big-leaf and "correct but useless" multilayer models (Bonan et al., 2021). The former model lacks the physically-sound foundations of the latter, but is more computationally efficient, do not require excessive data to implement, and provide reasonably acceptable estimates. On the other hand, complexity of multilayer models can be reduced by decreasing the number of canopy layers (Bonan et al., 2021).

In forest environments, the comparison of canopy photosynthesis obtained by upscaling leaf data with measurement obtained using Eddy Covariance revealed that big-leaf models systematically underestimated carbon gain (40–70 %) unless at least shaded leaves are independently parametrized (sun-shade models) (Sprintsin et al., 2012). Indeed, introducing a vertical gradient in the canopy by increasing the number of canopy layers further increases the accuracy. Very limited information about photosynthetic traits of urban tree species is available and it is mostly limited to full-sun leaves. Evaluating the accuracy of big leaf, compared to sun-shade and multilayer models at urban sites, is crucial to assess whether available data on full sun leaves may yield acceptable estimates of $CO_2$ assimilation by the urban canopy without the need of conducting extensive measurements to characterize photosynthetic traits of shade leaves along the vertical canopy gradient.

Using two European cities as living laboratories, 1) $CO_2$-assimilation per unit leaf area by 15 woody species growing in parks or along streets was quantified through the measurement of instantaneous and daily leaf gas exchange on about 17,000 leaves from 450 individual trees; 2) canopy traits were measured to upscale $CO_2$-assimilation per unit leaf area to the crown-projection area and to the whole plant using both big-leaf and multilayer approaches; 3) $CO_2$-sequestration and storage were measured by TLS LiDAR and compared to whole plant $CO_2$-assimilation. Such activities were carried out to test the specific research hypotheses that: 1) photosynthetic rate differs among species under average urban

conditions and is a major determinant of overall plant $CO_2$-uptake; 2) street trees provide similar $CO_2$-assimilation as park trees (Fini et al., 2022), unless specific management issues (e.g. heavy pruning) occur; 3) $CO_2$-sequestration underestimates the net removal of atmospheric $CO_2$ by urban vegetation; 4) canopy photosynthesis is underestimated by the big-leaf, compared to the multilayer model because shade-acclimation is ignored.

## 2. Methods

### 2.1. Experimental sites and plant material

The research was conducted in Rimini (Italy) and Krakow (Poland). Rimini has a warm temperate climate with even distribution of rainfall and very hot summers (Cfa, according to Koppen-Geiger classification). The average minimum and maximum temperatures over the last 30 years are 8,6 °C and 17,6 °C, respectively, and average rainfall is 705 mm per year. Krakow has a temperate climate with features of both European marine west coast and continental conditions of Eastern Europe (Cfb). Average minimum and maximum temperatures over the last 30 years are 3,8 °C and 12,8 °C, respectively, and average rainfall is 662 mm per year. Rainfall and potential evapotranspiration ($ET_0$) measured over the experimental period (2018–2021) are reported in Fig. A.1 in supplemental material. Weather data were obtained using UBIMET, a commercial weather data provider. UBIMET operates its own high-resolution weather model fed hourly with the latest weather data (precipitation radar, VERA analyses, lightning, satellite data, aircraft altitude profiles) to provide spatially and temporally highly accurate weather forecasts worldwide for a wide range of industries. Based on UBIMET data, $ET_0$ was calculated using the Penman-Monteith equation modified by FAO (Allen et al., 1998). In addition to climate, major differences between cities included population density (2-fold higher in Krakow than in Rimini), air particulate matter concentration (PM10 was 48 % higher in Krakow than in Rimini), for the design (mostly mono-specific and even-aged in Rimini; mostly pluri-specific, with shared rooting space and uneven-aged in Krakow), and for management practices of street trees (pruning in particular, see below).

The experimental areas were selected in different neighbourhoods of the two cities where full tree inventories had been conducted (Fig. A.2). In Rimini, the experimental area size was 250 ha and hosted about 44,680 inventoried trees from 84 species, although 20 species from 10 genera accounted for about 75 % of tree population. In Krakow, the experimental area was an east-west city transect of 472 ha which hosted about 50,073 inventoried trees from 73 species, although 50 % of total tree population was made by 14 species from 5 genera. A detailed list of locations included in the experimental areas is provided in Appendix 1.

The experimental areas were stratified into paved (street trees, trees in parking lots) and unpaved (park trees) strata. Routinary tree management activities were retrieved in the database of the two municipal tree care companies, Anthea and ZZM, which have long overseen management of green areas in Rimini and Krakow, respectively. According to municipal standards, trees growing in unpaved sites were subjected to minimal pruning (cleaning only) in both cities. Street trees were pruned with a 5-year cycle, using a mild (Krakow, structural defects highly tolerated by municipality and population) or severe (Rimini, frequent use of topping) pruning intensity. Estimates of pruning intensity of street trees, calculated as the ratio between crown projection area of each pruned street and crown projection area of an unpruned park tree of equal stem diameter, is reported in Fig. A.3. In Krakow only, de-icing salts were ordinarily used along streets during winter, while no use of de-icing salts was reported in parks. Consistently, soil samplings conducted by the municipality at the end of winter revealed a transient increase in extractable $Na^+$ (1.51 meq/100 g) recorded for street trees but not for park trees (extractable $Na^+$ = 0.03 meq/100 g). Extractable Na + in soil along street recovered to 0.05 0.03 meq/100 g in fall. Irrigation is manually performed in both cities, for 4 (Rimini) and 3

(Krakow) years after planting, on a regular schedule (Rimini) or when visible wilting appears (Krakow). After such period, no irrigation is performed on both park and street trees in both cities.

Eight tree and one shrub species per city were selected based on their relevance in the existing tree inventories, their even distribution in the cities, and on their final size at maturity. The list of species and their abbreviations and shade tolerance, the number of trees on which growth traits were assessed, and their minimum and maximum diameter are reported in Table 1. *Aesculus hippocastanum (Ah)*, *Populus nigra* 'Italica' *(Pn)*, and *Quercus robur (Qr)* were selected in both cities, although *Qr* plants differed for growing habit between the two cities (cultivar 'Pyramidalis' in Rimini; wild-type in Krakow). Two genera (*Acer, Tilia*) co-occurred in the two cities, although different species were selected: *A. negundo (An)* and *T. x europaea (Te)* in Rimini; *A. platanoides (Ap)* and *T. cordata (Tc)* in Krakow. Selected trees were marked with a unique identifier using ArboTag (R3Gis, Italy).

### 2.2. Dendrometric traits and Leaf Area Index

Planting date of selected trees was retrieved from municipal archives (e.g. date of site construction, data records about new tree plantings and maintenance activities) in both cities, and time after planting was calculated in years as the actual year – year of planting. All trees selected for this research had been planted >5 years before the onset of the experiment and were considered fully established. 737 and 975 combined measurements of DBH, plant height, and crown radius were performed in Rimini and Krakow, respectively. Stem circumference of tree species was measured at 1.35 m height using a measuring tape and DBH was calculated from circumference. For shrubs (*Ca* and *Pl*) which were often multi-stemmed, diameter was measured at the highest possible point to take a single trunk measurement below any swelling in stem taper due to forking (Magarik et al., 2020). Canopy radius was measured on all plants using a laser rangefinder (Metrica, Italy) according to the vertical sightseeing method, upon calibration using a plummet (Pretzsch et al., 2015). Crown projection area (CPA, $m^2$) was calculated from the quadratic mean of canopy radius ($R_{crown}$, m) as: $CPA = R_{crown}^2 * \pi$. Plant

**Table 1**
Species selected in the experimental areas of Rimini and Krakow, number of plants on which DBH was measured, and minimum and maximum DBH observed. st and sr in brackets after species name denote shade-tolerant and sun-requiring species, respectively.

| Species | Abbreviation | n. | DBH min. (cm) | DBH max. (cm) |
|---|---|---|---|---|
| Rimini | | | | |
| *Acer negundo* L. (st) | *An* | 80 | 7.50 | 67.62 |
| *Aesculus hippocastanum* L. (sr) | *Ah* | 105 | 5.00 | 76.43 |
| *Ligustrum lucidum* Aiton (st) | *Ll* | 76 | 8.00 | 30.90 |
| *Platanus x acerifolia* (Aiton) Willd. (sr) | *Pa* | 78 | 5.30 | 77.55 |
| *Populus nigra* L. 'Italica' (sr) | *Pn* | 78 | 7.50 | 92.36 |
| *Prunus laurocerasus* L. (st) | *Pl* | 12 | 4.00 | 37.88 |
| *Quercus ilex* L. (st) | *Qi* | 110 | 11.50 | 109.18 |
| *Quercus robur* L. 'Pyramidalis' (sr) | *Qr* | 89 | 8.00 | 51.43 |
| *Tilia x europaea* L. (st) | *Te* | 109 | 6.20 | 58.93 |
| | | | | |
| Krakow | | | | |
| *Acer platanoides* L. (st) | *Ap* | 135 | 5.00 | 84.39 |
| *Aesculus hippocastanum* L. (sr) | *Ah* | 125 | 4.50 | 109.71 |
| *Cornus alba* L. (st) | *Ca* | 29 | 2.23 | 8.46 |
| *Fraxinus excelsior* L. (st) | *Fe* | 128 | 4.50 | 84.87 |
| *Populus nigra* L. 'Italica' (sr) | *Pn* | 96 | 7.00 | 96.80 |
| *Quercus robur* L. (sr) | *Qr* | 126 | 5.00 | 129.14 |
| *Sorbus aucuparia* L. (st) | *Sa* | 103 | 4.00 | 50.64 |
| *Tilia cordata* Mill. (st) | *Tc* | 146 | 5.00 | 74.73 |
| *Ulmus laevis* Pall. (st) | *Ul* | 87 | 4.00 | 118.15 |

height was measured using a clinometer (SUUNTO, Vantaa, Finland).

Canopy transmittance to photosynthetically active radiation ($\tau$) and the fractional beam ($f_b$, i.e. the ratio of direct light vs. light coming from other sources) were measured using the Accupar ceptometer (Accupar LP-80, Decagon Devices, Washington, USA) during bright days (PAR > 1300 μmol m$^{-2}$ s$^{-1}$ and progressive change in PAR < 75 μmol m$^{-2}$ min$^{-1}$) in May, June, and July 2019–2021 (leaf on). Measurements were conducted between 11.30 and 14.30 to minimize solar zenith angle variation among treatments (De Mattos et al., 2020), on the same trees on which instantaneous CO$_2$ assimilation was measured (198 and 252 plants in Rimini and Krakow, see Section 2.3.1 for further details). Canopy transmittance and $f_b$ were also measured in February 2020–2021 (leaf off) on 6 (Rimini) and 7 (Krakow) replicates per species and strata (72 and 84 plants in total in Rimini and Krakow, respectively). Isolated trees were sub-sampled among those on which $\tau$ was measured during summer for the $\tau$ leaf off measurement. Four readings of above-canopy irradiance (S) (measured by positioning the ceptometer horizontally at about 1 m above the canopy, which was accessed using the basket elevator) and below-canopy irradiance (measured about 1 m below the lower edge of the canopy) were collected per plant (Leblanc and Chen, 2001; Sharma et al., 2018).

The true Leaf Area Index (LAI, half of total leaf area per unit horizontal ground area, m$^2$ m$^{-2}$) was calculated from $\tau$ using a simplification of the model proposed by Norman and Jarvis (1975), after correcting the measured values for woody area index and clumping (Yan et al., 2019):

$$LAI = (1 - \alpha) * \{\{[1 - (1/2\,K) * f_b] - 1\} * ln\tau\} / [Abs^* (1 - 0,47^* f_b)]^* (\gamma/\Omega)$$

where: $\alpha$ is the ratio between the true Woody Area Index and the true Plant Area Index, K is the directional light extinction coefficient calculated according to Campbell (1986) taking into account the species-specific leaf insertion angles (Chianucci et al., 2018; Boni Vicari et al., 2019; Hagemeier and Leuschner, 2019), Abs is canopy absorbance (set as 0.86, De Mattos et al., 2020), $\gamma$ is within shoot clumping which is 1 for broadleaves, and $\Omega$ is clumping index. A full description of the equations and methods used for LAI calculation is reported in Appendix 1.

### 2.3. Net CO$_2$ assimilation per unit leaf area

#### 2.3.1. Instantaneous measurements on full sun leaves

Net CO$_2$-assimilation per unit leaf area at saturating irradiance (A$_{sat}$, μmol m$^{-2}$ s$^{-1}$) was measured on 3 fully-expanded leaves per plant. Only leaves exposed to full solar irradiance and located in the outermost portion of the apical, medial, and basal portions of the canopy were sampled. To access the canopy, a basket elevator (NT400, Nissan, Japan) was used. Measurements were conducted using an infrared gas-analyser (LICOR 6400, Li-Cor, Lincoln, NE, USA), by supplying the leaves with 420 ppm CO$_2$ and 1300 μmol PAR m$^{-2}$ s$^{-1}$ according to well established protocols (Fini et al., 2015, 2022). Measurements were conducted on 11 replicate plants per species and strata (198 plants in total) in Rimini and on 14 replicate plants per species and strata (252 plants in total) in Krakow.

Plants were selected according to the following criteria: 1) be representative of the different DBH classes displayed by the individual species in each city; 2) be established in the planting site (> 5 years from planting date); 3) be isolated, in rows, or in the outer portion of small groups of trees, with most of the canopy unshaded by other trees; 4) occur in locations where even-aged plants of the same species could be found as both park and street trees; 5) occur in location where individuals of other measured species were planted within a small distance. A detailed list of individual plants sampled for A$_{sat}$ measurement is provided in Appendix 1.

Measurements were conducted during spring (Rimini: mid-May 2019; Krakow: early-June 2019), summer (Rimini: late-July 2018; Krakow: late-July 2019), and fall (Rimini: early-October 2018; Krakow: late-September 2018). Measurements were conducted over multiple

days, from 9.00 to 13.00 and from 14.00 to 17.45, having care to randomize the species and strata among the different days and time of measurement. Additional instantaneous measurements of A$_{sat}$ were carried out on 8 replicate plants of *An, Pa, Pl* in Rimini and *Ca, Fe, Sa* in Krakow during fall 2019 (Krakow: late-September); summer 2020 (Rimini: early July; Krakow: late-July), spring 2021 (Rimini: mid-May; Krakow: early June) and fall 2021 (Rimini: early-October).

#### 2.3.2. Daily measurements on full sun and shaded leaves

Daily measurements of CO$_2$-assimilation were conducted on 8 mature (DBH > 18 cm) plants per strata and species from 6 of the 9 species screened with the instantaneous measurements (96 plants per each sampling date and city). Plants were subsampled by selecting in each replicate area those individuals with A$_{sat}$ closer to the species average in each stratum. Measurements were performed on 4 fully expanded leaves per plant (1152 leaves per city and sampling date; 6912 leaves per city measured over the entire experiment). Leaves were selected after was ideally dividing the canopy in two layers across its vertical profile: an apical (a) and a basal (b) layer, accounting each for 50 % of live canopy height. Within each layer, one external leaf, fully exposed to solar irradiance (ae and be denote full-sun leaves sampled in the apical and basal layer of the canopy, respectively) and one leaf internal to the canopy and subjected to self-shading (ai and bi denote shaded leaves sampled in the apical and basal layer of the canopy, respectively) were measured. Measurements were carried on the same tree over multiple time-points per day: morning (9.15–11.30; A$_{mor}$, μmol m$^{-2}$ s$^{-1}$), midday (12.45–15.00; A$_{midd}$), afternoon (16.00–18.15; A$_{aft}$), and nigh-time (23.00–01.00; R$_{dark}$).

Measurements were conducted by exposing the leaf into the Licor-6400 cuvette to 420 ppm CO$_2$ and an irradiance, provided using the integrate LED, which mimicked the average PAR experienced by each leaf class during each day-fraction and season. CO$_2$-assimilation of ae and be leaves was measured at a PAR$_{sun}$ in the cuvette set equal to the average above-canopy PAR (S) recorded by Ubimet between 9.00 and 11.30 (for morning measurements), between 12.45 and 15.00 (for midday measurements) and between 16.00 and 18.15 (for afternoon measurements) over the last 15 sunny days before each measurement campaign. CO$_2$-assimilation of ai and bi leaves was measured at a PAR$_{shade}$ = S * $\tau$ where $\tau$ is transmittance in the apical ($\tau_{Ai}$) and basal ($\tau_{Bi}$) layers of the canopy (Table A.1 in supplemental material). To measure $\tau_{Ai}$ and $\tau_{Bi}$, the ceptometer was firstly positioned horizontally at about 1 m above the canopy, as previously described. Then, it was positioned horizontally within the canopy, at a height corresponding to about half of the height of each layer and at a horizontal distance from the canopy edge corresponding to about 30 % of live crown radius (e.g. the fraction of canopy radius densely covered with foliage) (Sharma et al., 2018). PAR was set equal to 0 for R$_{dark}$ measurements.

Daily measurements were conducted during spring (Rimini: late-May 2019, mid-May 2021; Krakow: early-June 2019; mid-June 2021), summer (Rimini: early-July 2019, early-July 2020; Krakow: late-July 2019, late-July 2020), and fall (Rimini: mid-October 2018, early-October 2021; Krakow: late-September 2019; late-September 2020). Due to time limitation and the need to complete the measurement of each replicate within a day, daily measurement on *An, Pl, Pa* (Rimini) and on *Ca, Fe,* and *Sa* (Krakow) were only performed in 3 measurement campaigns carried out between 2018 and 2019.

The daily amount of CO$_2$ assimilated by the unit leaf area (A$_{daily}$, g CO$_2$ m$^{-2}$ day$^{-1}$) of ae, ai, be, and bi leaves was estimated as the integral of A$_{mor}$, A$_{mid}$, A$_{aft}$, and R$_{dark}$ of each leaf position over the whole day (Fini et al., 2014; Mori et al., 2016).

### 2.4. Canopy CO$_2$-assimilation

CO$_2$-assimilation per unit leaf area was upscaled to the unit crown projection area and to the whole tree using a big leaf and a multilayer approach (Luo et al., 2018; Bonan et al., 2021).

### 2.4.1. Big-leaf model

According to the big-leaf approach, $CO_2$-assimilation per unit crown projection area ($A_{cpaBL}$, $\mu mol\ m^{-2}$ ground $s^{-1}$) was calculated as (De Pury and Farquhar, 1997): $A_{cpaBL} = A_{sat}*(1 - e^{-k*\Omega*LAI})/k$.

Where: $A_{sat}$ is instantaneous net $CO_2$-assimilation of full sun leaves ($\mu mol\ m^{-2}\ s^{-1}$), k is the extinction coefficient for PAR and leaf nitrogen gradients within the canopy, set as 0.5, LAI and $\Omega$ are the true Leaf Area Index and clumping index.

$CO_2$-assimilation per unit crown projection area over the whole day ($A_{cpaBL(d)}$, g $m^{-2}$ ground $day^{-1}$) was calculated as: $44*10^{-6}*(A_{cpaBL}*n.$ $seconds_{dawn\ to\ dusk} - R_{cpa}*n.\ seconds_{dusk\ to\ dawn})$, where $R_{cpa}$ ($\mu mol\ m^{-2}$ ground $s^{-1}$), i.e. the $CO_2$ released at night-time by the unit crown projection area, was calculated as: $R_{cpa} = R_{dark}*LAI$.

### 2.4.2. Multilayer sun-shade model

According to the multilayer approach, $CO_2$-assimilation per unit crown projection area ($A_{cpaML}$, $\mu mol\ m^{-2}$ ground $s^{-1}$) was calculated separately in each season for morning, midday, and afternoon as (Luo et al., 2018):

$$A_{cpaML,\ mor/mid/aft} = 0.5^* \left( A_{ae,mor/mid/aft}{}^*LAI_{sun} + A_{ai,mor/mid/aft}{}^*LAI_{shade} \right)$$
$$+ 0.5^* \left( A_{be,mor/mid/aft}{}^*LAI_{sun} + A_{bi,mor/mid/aft}{}^*LAI_{shade} \right)$$

where: $A_{ae}$, $A_{ai}$, $A_{be}$, and $A_{bi}$ are net $CO_2$-assimilation ($\mu mol\ m^{-2}\ s^{-1}$) by ae, ai, be, and bi leaves during the morning (mor), at midday (mid), or during the afternoon (aft) in spring, summer, and fall (see Table A.2 for full data); $LAI_{sun}$ and $LAI_{shade}$ are the fractions of LAI exposed to full solar irradiance and self-shaded, respectively, assessed on hourly basis; 0.5 assumes equal distribution of leaf area between the apical and basal canopy layers.

LAI was partitioned into its sun and shaded fractions as previously described (Luo et al., 2018):

$$LAI_{sun} = 2cos\theta^* \left( 1\ - e^{-0.5^*\Omega^*LAI/cos\theta} \right)$$

and

$$LAI_{shade} = LAI - LAI_{sun}$$

where $\theta$ is solar zenith angle (rad).

The net amount of $CO_2$ removed per unit crown projection area in a day ($A_{cpaML(d)}$, g $m^{-2}$ ground $day^{-1}$) was calculated in each season as: $A_{cpaML(d)} = 44*10^{-6}*(\int_1^{n,mor} A_{cpa,mor} + \int_1^{n,mid} A_{cpa,mid} + \int_1^{n,aft} A_{cpa,aft} - \int_1^{86400-n,day} R_{cpa})$, where $n_{,mor}$ is the number of seconds from sunrise to 11.30; $n_{,mid}$ between 11.30 and 16.00; $n_{,aft}$ between 16.00 and sunset; and $n_{,day} = n_{,mor} + n_{,mid} + n_{,aft}$.

For species on which daily measurements were not performed during the whole experimental period (*An*, *Pl*, and *Pa* in Rimini; *Ca*, *Fe*, and *Sa* in Krakow), $A_{cpaML(d)}$ was calculated as $A_{cpaBL(d)}/s$, where s is the species-specific slope of relationship between $A_{cpaBL(d)}$ and $A_{cpaML(d)}$ measured in the period 2018–2019 (see Table A.3 in supplemental materials).

Daily $CO_2$-assimilation by the whole tree ($A_{tree(d)}$, kg $tree^{-1}\ day^{-1}$) was calculated as $A_{cpaML(d)}*CPA$ (Rötzer et al., 2019). To allow the comparison with $CO_2$-sequestration, annual $CO_2$-assimilation by the whole tree ($A_{tree(y)}$, kg $tree^{-1}\ year^{-1}$) was estimated using the GREEN-SPACES software as the sum of $A_{cpaML(d)}$ measured in spring (full leaf expansion to 20th June), summer (21st June to 20th September), and fall (21st September to leaf yellowing) assuming $A_{cpa,mor/mid/aft} = 0$ during hours when average $S < 115\ \mu mol\ PAR\ m^{-2}\ s^{-1}$.

### 2.5. CO₂-storage and sequestration

The volume of trunk and main branches ($V_{abg}$, $m^3$) was estimated using a TLS LiDAR (RIEGL, Horn, Austria) on the same trees used for leaf gas exchange measurements. The TLS point clouds (class = 1) representing trees scanned in the leafless period were processed using TreeQSM software (Matlab environment, Version 2.4.0, Pasi Raumonen©, https://github.com/InverseTampere/TreeQSM) which enabled the 3D-modelling and reconstruction of tree structure according to the Quantitative Structure Models (QSM's) approach (Raumonen et al., 2013). The QSM model consists of a hierarchical collection of digital CAD cylinders estimating topological, geometrical and volumetric objects (parts) of the woody structure of the single tree. The volume of the main trunk and of individual branches were estimated using the QSM approach and summed to obtain $V_{abg}$. More details about the TLS methods and the QSM approach are reported in Appendix 1.

$CO_2$-storage (kg $CO_2\ tree^{-1}$) was calculated from $V_{abg}$ as:

$$CO_{2storage} = 1.28^*3.667^*0.5^*V_{abg}{}^*\rho$$

where 1.28 is a coefficient to account for root biomass (Aguaron and McPherson, 2012), 3.667 is the conversion factor between carbon and $CO_2$, 0.5 accounts for half of plant dry biomass being made of carbon, and $\rho$ is dry density (dry weight/fresh volume) (Picard et al., 2012). $\rho$ for the different species were retrieved in Zanne et al. (2009) and Wilcox (2000). $CO_2$-density (kg $m^{-2}$ ground) was calculated as: $CO_{2storage}/CPA$ (Nowak, 1994).

$CO_2$-sequestration (kg $CO_2\ tree^{-1}\ year^{-1}$) was calculated using age-DBH and DBH-volume curves (see Statistics section) as the increase in $CO_{2storage}$ over one growing season (Nowak and Crane, 2002). Stem DBH before the beginning and after the end the growing season were estimated imposing consecutive years as input variable in age-DBH curves. $CO_{2storage}$ before the beginning and after the end of the growing season were calculated using DBH-volume from the corresponding DBH. Finally, $CO_2$-sequestration was calculated as the difference between $CO_{2storage}$ after the end of the growing season and $CO_{2storage}$ before sprouting.

### 2.6. Statistics

The experimental design was a split-plot where strata was the main-plot and species the sub-plot. All statistics have been carried out using the SPSS statistical package (IBM, Version 21.0. Armonk, NY, USA). To evaluate the effects of species, strata, leaf position, season, and their interactions on instantaneous $CO_2$-assimilation, a mixed-model procedure was applied. Because a significant species x strata x season interaction was found for both cities, species and seasons were compared independently per each stratum (e.g. park and street). Daily $CO_2$-assimilation was analysed using a nested mixed model where leaf position nested within species and strata were considered as fixed factors and season as random factor. Because a significant position(species) x strata interaction was found in both cities, $A_{daily}$ was analysed separately per each species. A machine learn approach (automatic linear model) was used to identify if species, stratum, and stem diameter were significant predictors of plant age, Cr, LAI, $V_{abg}$, $A_{sat}$, and of the ratio between $CO_2$-sequestration and assimilation. Age-DBH, DBH-Cr, DBH-volume of trunk and main branches, and DBH-$A_{sat}$ curves were fitted using the curve fitting tool included in SPSS. The allometric curves were constrained to a maximum of 65-years to avoid extrapolation of data beyond the maximum age class which was broadly represented by the dataset. Linear, power, sigmoid, and logarithmic functions were used for fitting. Tree height was not considered a reliable predictor of other tree attributes because it can be suddenly and drastically affected by management practices (e.g. pruning) in urban sites. A linear regression was used to test the relationship between $A_{cpaML}$ and $A_{cpaBL}$.

## 3. Results

### 3.1. Growth and Leaf Area Index

Time after transplanting and species were significant predictors of DBH ($P < 0.001$; $R^2 = 0.816$ and $0.737$ in Rimini and Krakow,

respectively) while stratum was not (P > 0.05). The power function (DBH = b*Age$^a$) best fitted the observed data for all species except for *Sa*, where the best fit was achieved by a sigmoid function (Table 2). When power functions were used to estimate DBH, the exponent averaged 0.83 in Rimini and 0.88 in Krakow.

DBH, species, and strata were significant predictors of crown radius (Cr, P < 0.001; R$^2$ = 0.698 and 0.715 in Rimini and Krakow, respectively), therefore allometric equations are presented separately for park and street trees in Table 2. The best fit was achieved through the power function Cr = b*DBH$^a$ for all species and strata. The exponent a of park trees averaged 0.752 and 0.707 in Rimini and Krakow, respectively, while a of street trees averaged 0.709 (Rimini) and 0.683 (Krakow).

DBH and species (P < 0.01) but not strata (P > 0.05) were significant predictors of above-ground volume (V$_{abg}$, R$^2$ = 0.710 and 0.778 in Rimini and Krakow, respectively). The best fit was achieved through a sigmoid function V$_{abg}$ = e$^{((b+(a/DBH))}$ for all species and strata except for the shrub species *Ca* which best conformed to a linear fit (V$_{abg}$ = b + a*DBH) (Table 2).

DBH was a poor predictor of the true LAI (P > 0.05; R$^2$ = 0.06) which, instead, was affected by a significant species x strata interaction in both cities (P < 0.01). In Rimini, *Ah*, *Pl*, and *Pa* growing in parks displayed higher LAI than *Ll* and *Qr* (Fig. 1A). *An* and *Pl* growing along streets displayed higher LAI than other species. Park trees of *Ah*, *Pa*, *Pn*, *Pl*, *Qi* and *Qr* had, on average, 19.2 % higher LAI compared to their street counterparts. On the contrary, strata did not affect LAI in *An*, *Ll*, and *Te*. Among park trees of Krakow, *Ah* displayed higher LAI than other species (Fig. 1B). In streets, *Ca* displayed higher LAI than other species. *Sa* displayed, in general, lower LAI than other species in both parks and along streets. *Ap*, *Ah*, *Qr*, and *Ul* had, on average, 13.3 % higher LAI when grown in parks compared to streets. Conversely, *Ca* growing along streets had 51.1 % higher LAI compared to parks.

### 3.2. Instantaneous CO$_2$ assimilation by full sun leaves

In Rimini, during spring, park trees of *Pn*, *Qr*, *Ah*, and *Te* displayed higher A$_{sat}$ than *An* and *Ll* (Fig. 2A; Table A.4 in supplemental material). A$_{sat}$ of park trees of *Pa* (−50.7 %), *Ah* (−41.6 %), *Pl* (−41.6 %), and *Te* (−32.2 %) declined steeply from spring to summer. A$_{sat}$ of park trees did not recover in fall, except for *Pa* (+36.5 % in fall compared to summer). Park trees of *Ll*, *Qi* and *Qr* maintained similar A$_{sat}$ throughout the year. Street trees of *Pn*, *Qr*, and *Te* displayed higher A$_{sat}$ than other species

during spring (Fig. 2B). A$_{sat}$ increased from spring to summer in street trees of *Pn* (+43 %) and *Qi* (+36 %). Conversely, *Pa* (−26 %), *Te* (−26 %), and *Pl* (−25 %) displayed lower A$_{sat}$ in summer, compared to spring. During fall, A$_{sat}$ of street trees was either similar (*Ll*, *Pl*, *Qi*, *Qr*, *Te*) or lower (*Ah*, *An*, *Pn*) compared to summer values.

In Krakow, A$_{sat}$ of park trees did not differ between spring and summer in any species except for *Sa*, which displayed 48 % lower A$_{sat}$ in summer, compared to spring (Fig. 2C; Table A.4). During fall, park plants of all species except *Ca* displayed lower A$_{sat}$ than during spring, although such decline was steeper in *Ah* (−54 %), *Fe* (−44 %), and *Ap* (−42 %) compared to *Tc* (−23 %) and *Pn* (−14 %). During spring and summer, street trees of *Pn* displayed higher A$_{sat}$ compared to *Fe* and *Qr* which, in turn, displayed higher A$_{sat}$ than *Ap*, *Sa*, and *Tc* (Fig. 2D). Street-grown *Pn* and *Qr* displayed 27 % and 21 % higher A$_{sat}$ in summer compared to spring. Conversely, *Ah* displayed 20 % lower A$_{sat}$ in summer, compared to spring. During fall, A$_{sat}$ of street-grown *Ap*, *Ah*, and *Fe* was 42 %, 66 %, and 36 % lower compared to spring.

In both cities, leaves of all species attached on basal branches displayed lower A$_{sat}$ compared to leaves attached on medial and apical branches (data not shown). Significant correlations between DBH and Asat were found neither in Rimini (P = 0.179) nor in Krakow (P = 0.895) (data not shown).

### 3.3. Daily CO$_2$ assimilation in full-sun and shaded leaves

The average daily CO$_2$-assimilation by full sun leaves of both the apical and basal canopy layers (A$_{daily,ae}$ and A$_{daily,be}$) was higher in *Pn* and *Qr* compared other species in both cities (Fig. 3; Table A.5 in supplemental material).

In Rimini, A$_{daily,ae}$ of *Ah* growing in parks was higher than in street trees (Fig. 3A). Conversely, street trees of *Ll*, *Qr*, and *Qi* displayed higher A$_{daily,ae}$ than park trees (Fig. 3F, G, I). CO$_2$ assimilation by shaded leaves of the apical canopy layer (A$_{daily,ai}$) was lower than A$_{daily,ae}$ in all species, with smaller differences observed in *Ll* (−43 %, Fig. 3F) and larger differences found in *Qr* (−57 % compared to ae leaves, Fig. 3G). CO$_2$ assimilation by shaded leaves of the basal canopy layer (A$_{daily,bi}$) was, on average, 65 % lower than A$_{daily,be}$, with larger reductions observed in *Te* (−74 %), *Qi* (−81 %) and *Qr* (−82 %) (Fig. 3L, G, I). Strata little affected carbon gain of Bi leaves.

In Krakow, strata did not affect the annual average A$_{daily,ae}$ and A$_{daily,be}$, except for *Ap* and *Pn* (Fig. 3C, E). A$_{daily,ai}$ was about was on average

**Table 2**
Wellness of fit (R$^2$) and empirical coefficients (a and b) to fit the allometric relationships to estimate: 1- Stem diameter at breast height (tree species) or at the lowest fork (shrub species) (DBH, cm) from time after transplant (Age, years); 2- crown radius (Cr, m) from DBH (cm) in park and street trees, and 3- above-ground volume (V$_{abg}$, m$^3$) from DBH (cm) in a Cfa (Rimini) and Cfb (Krakow) climate. V$_{abg}$ was not determined (N.D.) on evergreen species. DT = deciduous tree; DS = deciduous shrub; ET = evergreen tree; ES = evergreen shrub.

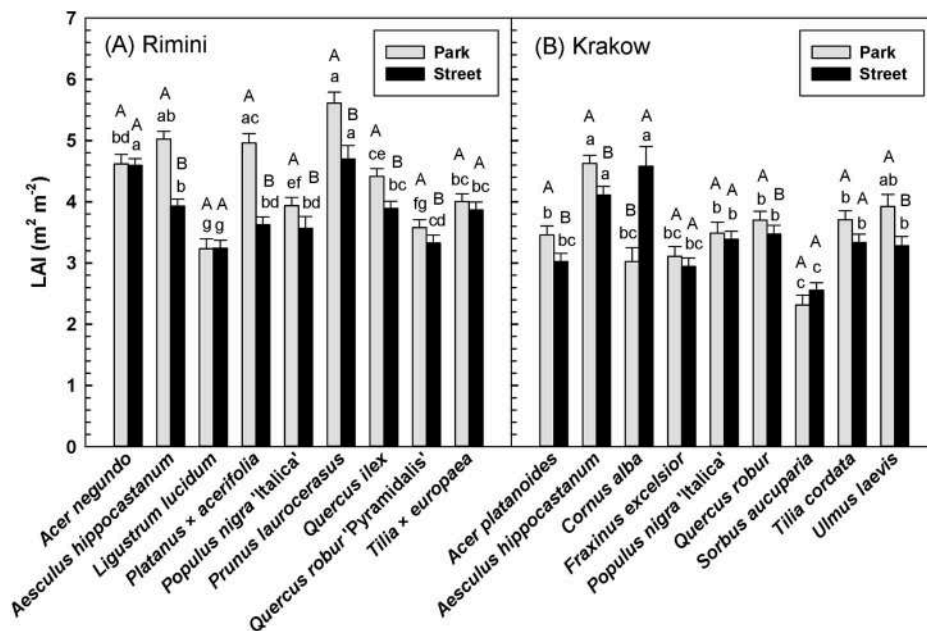| Species | City | DBH = b*Age$^a$ or DBH = e$^{((b+(a/age))}$ (*S. aucuparia*) | | | Cr = b*DBH$^a$ (park trees) | | | Cr = b*DBH$^a$ (street trees) | | | V$_{abg}$ = e$^{((b+(a/DBH))}$ or V$_{abg}$ = b + a*DBH (*C. alba*) | | |
|---|---|---|---|---|---|---|---|---|---|---|---|---|---|
| | | a | b | R2 | a | b | R2 | a | b | R2 | a | B | R2 |
| *A. negundo* (DT) | Rimini | 0.9240 | 1.1139 | 0.883 | 0.9056 | 0.1955 | 0.756 | 0.5763 | 0.3973 | 0.634 | -35,77 | 1653 | 0,884 |
| *A. platanoides* (DT) | Krakow | 0.7990 | 1.8168 | 0.873 | 0.7491 | 0.3184 | 0.871 | 0.7491 | 0.3184 | 0.871 | −29,49 | 1966 | 0,947 |
| *A. hippocastanum* (DT) | Rimini | 0.9996 | 0,9590 | 0.947 | 0.8098 | 0.2356 | 0.789 | 0.6053 | 0.3366 | 0.873 | −33,65 | 0,942 | 0,831 |
| *A. hippocastanum* (DT) | Krakow | 0.9187 | 1.5088 | 0.896 | 0.6772 | 0.3467 | 0.947 | 0.5007 | 0.6290 | 0.376 | −117,06 | 3269 | 0,930 |
| *C. alba* (DS) | Krakow | 1.0627 | 0.2522 | 0.847 | 0.6368 | 0.4052 | 0.903 | 0.4666 | 0.4981 | 0.613 | 0,046 | −0,170 | 0,994 |
| *F. excelsior* (DT) | Krakow | 1.1137 | 0.7448 | 0.942 | 0.9197 | 0.1482 | 0.913 | 0.7910 | 0.2817 | 0.746 | −63,73 | 2794 | 0,639 |
| *L. lucidum* (ET) | Rimini | 0.4507 | 3.5630 | 0.416 | 0.5777 | 0.3006 | 0.289 | 0.3381 | 0.5105 | 0.306 | N.D. | N.D. | N.D. |
| *P. x acerifolia* (DT) | Rimini | 1.1462 | 0.6502 | 0.858 | 0.8212 | 0.2654 | 0.905 | 0.6915 | 0.2910 | 0.863 | −69,18 | 2603 | 0,918 |
| *P. nigra* 'Italica' (DT) | Rimini | 1.0084 | 1.2849 | 0.897 | 0.6756 | 0.1662 | 0.854 | 1.1093 | 0.0303 | 0.778 | −38,30 | 1699 | 0,936 |
| *P. nigra* 'Italica' (DT) | Krakow | 0.7047 | 4.2950 | 0.777 | 0.8464 | 0.0719 | 0.572 | 0.4997 | 0.2839 | 0.466 | −25,28 | 1930 | 0,957 |
| *P. laurocerasus* (ES) | Rimini | 0.6141 | 2.2546 | 0.468 | 0.6978 | 0.2830 | 0.340 | 0.6978 | 0.2830 | 0.340 | N.D. | N.D. | N.D. |
| *Q. ilex* (ET) | Rimini | 0.6628 | 2.9073 | 0.781 | 0.8016 | 0.2604 | 0.907 | 0.8592 | 0.1251 | 0.826 | N.D. | N.D. | N.D. |
| *Q. robur* 'Pyramidalis' (DT) | Rimini | 0.7582 | 2.1014 | 0.736 | 0.6342 | 0.4305 | 0.630 | 0.8792 | 0.1213 | 0.775 | −47,23 | 2266 | 0,920 |
| *Q. robur* (DT) | Krakow | 0.9786 | 1.2701 | 0.920 | 0.5339 | 0.6912 | 0.734 | 0.9455 | 0.1313 | 0.940 | −50,00 | 2629 | 0,715 |
| *S. aucuparia* (DT) | Krakow | −14.56 | 3.6582 | 0.745 | 0.7792 | 0.1579 | 0.872 | 0.7579 | 0.1323 | 0.687 | −40,90 | 1829 | 0,950 |
| *T. cordata* (DT) | Krakow | 0.8777 | 1.6516 | 0.767 | 0.6201 | 0.4390 | 0.825 | 0.8091 | 0.2049 | 0.921 | −50,51 | 2649 | 0,950 |
| *T. x europaea* (DT) | Rimini | 0.9031 | 1.5039 | 0.887 | 0.8404 | 0.2128 | 0.898 | 0.6275 | 0.3348 | 0.839 | −42,73 | 1941 | 0,955 |
| *U. laevis* (DT) | Krakow | 0.8536 | 1.7177 | 0.908 | 0.5970 | 0.4513 | 0.477 | 0.4866 | 0.6239 | 0.772 | −51,77 | 2845 | 0,893 |

**Fig. 1.** Average (± standard deviation) true Leaf Area Index (LAI, m$^2$ m$^{-2}$) of park and street trees of the selected species growing in Rimini (A) and Krakow (B). For each city, different uppercase letters indicate significant differences between park and street trees within each species at P < 0.01. Different small letters indicate significant differences among species, within each stratum, at P < 0.01.

51 % lower compared to A$_{daily,ae}$, with lower reductions observed in *Ul* (−41 %, Fig. 3N) and *Ap* trees growing along streets (−37 %, Fig. 3C) and larger reductions in *Qr* (−60 % compared to ae leaves, Fig. 3H). A$_{daily,bi}$ was, on average, 74 % lower compared to A$_{daily,be}$, with some species (*Qr*: −82 %; *Ah*: −79 %, Fig. 3B, H) showing higher reductions than others (*Ap*: −62 %, Fig. 3C).

Full data about net CO$_2$-assimilation of the different leaf fractions in the two strata, during morning, midday and afternoon in the different seasons are reported in Table A.2 in supplemental materials.

### 3.4. CO$_2$-assimilation per unit crown projection area and per tree

Daily CO$_2$-assimilation per unit canopy area estimated using the big leaf model (A$_{cpaBL(d)}$) was highly correlated with CO$_2$-assimilation per unit canopy area estimated using the multilayer model (A$_{cpaML(d)}$) in both cities (Rimini: P < 0.000; R$^2$ = 0.923; Krakow: P < 0.000; R$^2$ = 0.941). Overall, A$_{cpaBL(d)}$ underestimated A$_{cpaML(d)}$ to a greater extent in Rimini (−30.9 %) than in Krakow (−6.2 %) (Table A.3). The automated linear model also revealed that species was a significant predictor of the slope of the relationship between A$_{cpaBL(d)}$ and A$_{cpaML(d)}$ (P < 0.000). Lower slopes were found in *An* and *Pa* compared to *Ll*, *Pl*, and *Qr* (Table A.3 in supplemental materials).

In both cities, A$_{cpaML(d)}$ was affected by a significant species x strata interaction (Table A.6 in supplemental materials). In Rimini, park trees of *Pn* and *Pa* had higher A$_{cpaML(d)}$ than other species (Fig. 4). Street trees of *Pn*, *Pa*, and *Qr* had higher A$_{cpaML(d)}$ than *An*, *Ah*, *Ll*, and *Pl* (Fig. 4A). In Rimini, A$_{cpaML(d)}$ did not differ between park and street trees of the same species, except for *Ah*, which displayed 44.7 % higher A$_{cpaML(d)}$ when grown in parks compared to streets, and for *Ll*, which displayed 37.3 % lower A$_{cpaML(d)}$ when grown in parks, compared to streets. In Krakow, park trees of *Pn* and *Qr* had higher A$_{cpaML(d)}$ than other species (Fig. 4B). Street trees of *Pn* had higher A$_{cpaML(d)}$ than *Qr* which, in turn, had higher A$_{cpaML(d)}$ than other species. In Krakow, *Ap* and *Ul* had higher A$_{cpaML(d)}$ when grown in parks compared to streets (Fig. 4B). Conversely, *Ca*, *Fe*, and *Pn* had higher A$_{cpaML(d)}$ when grown in streets compared to parks.

Panels C, D, E, F in Fig. 4 show calculated daily CO$_2$-assimilation (A$_{tree(d)}$, kg tree$^{-1}$ day$^{-1}$) by park and street trees in Rimini and Krakow as affected by time after transplant over an arbitrary 65-year lifecycle.

In parks of Rimini, *Qr* had higher A$_{tree(d)}$ than the other species for 12 years since transplant (0.594 kg CO$_2$ tree$^{-1}$ day$^{-1}$ after 10 years from planting) (Fig. 4C). Thereafter, *Pa* (16.40 kg CO$_2$ tree$^{-1}$ day$^{-1}$ 65 years after planting) outcompeted other species growing in parks for CO$_2$ assimilation. Street trees of *Te* (0.368 kg CO$_2$ tree$^{-1}$ day$^{-1}$ after 10 from planting) displayed higher A$_{tree(d)}$ than other species for 15 years since transplant (Fig. 4E). Thereafter, *Pa* (on average 5.80 kg CO$_2$ tree$^{-1}$ day$^{-1}$ after 65 years from planting) had higher A$_{tree(d)}$ than other street tree species. *Pl* (0.33 kg CO$_2$ tree$^{-1}$ day$^{-1}$ on average over a 65-year life-cycle) and *Ll* (0.13 kg CO$_2$ tree$^{-1}$ day$^{-1}$ on average over a 65-year life-cycle) displayed lower A$_{tree(d)}$ than even-aged individuals of other species in both parks and streets. On average, A$_{tree(d)}$ of street trees was 16 % lower compared to park trees for newly established trees (5 years after planting) and up to 57 % lower for mature trees (65 years after planting) (Fig. 4C, E). An exception was made by mature trees of *Pn* (> 45 years after planting), which displayed 36 % higher A$_{tree}$ when mature trees were grown in streets compared to parks.

In Krakow, park trees of *Qr* had higher A$_{tree(d)}$ than other species throughout the whole lifecycle (Fig. 4D). A$_{tree}$ of *Qr* ranged from 1.01 kg CO$_2$ tree$^{-1}$ day$^{-1}$ (10 years after planting) to about 7.13 kg CO$_2$ tree$^{-1}$ day$^{-1}$ after 65 years. Mature trees (> 45 years after planting) of *Fe* ranked 2nd among park tree species for A$_{tree(d)}$, although A$_{tree(d)}$ of *Fe* was lower than those of *Ap*, *Ah*, *Ul*, and *Tc* during the first 40 years after transplanting. *Fe* and *Qr* also displayed higher A$_{tree(d)}$ than other species when planted along streets (on average 9.10 and 8.72 kg CO$_2$ tree$^{-1}$ day$^{-1}$ for ash and oak, respectively, 65 years after planting), although *Ap* showed higher A$_{tree}$ than other species for 18 years since transplanting (Fig. 4F). *Ca* (0.27 kg CO$_2$ tree$^{-1}$ day$^{-1}$ on average over a 65-year life-cycle) and *Sa* (0.18 kg CO$_2$ tree$^{-1}$ day$^{-1}$ on average over a 65-year life-cycle) displayed lower A$_{tree(d)}$ than other species in both streets and parks.

### 3.5. CO$_2$ storage and sequestration

CO$_2$-density differed among species in both cities, and a significant species x strata interaction was found in Rimini (Fig. 5A, B; Table A.6). In Rimini, CO$_2$-density was higher in street compared to park trees for all species except *Pn*. In parks, *Pn* had 8-fold higher CO$_2$-density than other
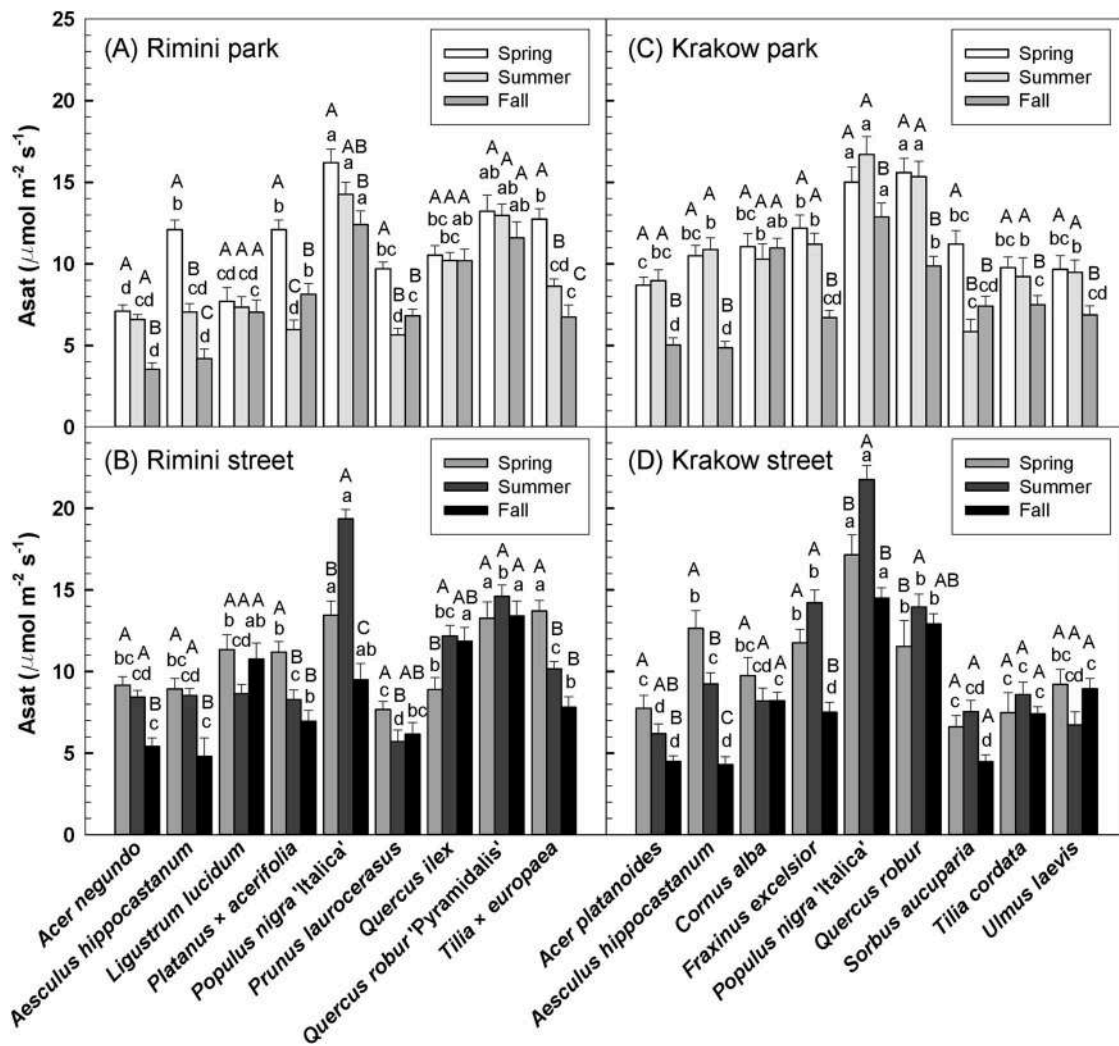
**Fig. 2.** Net $CO_2$-assimilation ($\pm$ standard deviation) measured at saturating light availability ($A_{sat}$, $\mu$mol m$^{-2}$ s$^{-1}$) during spring, summer, and fall by park (A, C) and street (B, D) trees of different woody species growing in Rimini (A, B) and Krakow (C, D). For each city, different uppercase letters indicate significant differences among season, within each species, at P < 0.01. Different small letters indicate significant differences among species, within each season, at P < 0.01.

species. In Krakow, strata did not affect $CO_2$-density, and *Pn* had 8-fold higher $CO_2$-density than most other species in both streets and parks.

$CO_2$-storage ($CO_{2stored}$, kg tree$^{-1}$) significantly scaled with DBH (Rimini: P < 0.000; R$^2$ = 0.911; Krakow: P < 0.000; R$^2$ = 0.888) following a sigmoid function, although species (P < 0.000) but not strata (P = 0.587 and P = 0.744 in Rimini and Krakow, respectively) affected the shape of the curve.

In Rimini, $CO_{2stored}$ by a late-mature specimen (e.g. 65 years after transplanting) ranged from 1750 kg $CO_2$ (*Ah*) to 7203 kg $CO_2$ (*Pa*) (Fig. 5C). Within 25 years since transplanting, *Qr*, *Te*, and *Pn* stored more $CO_2$ than *Pa*. In Krakow, $CO_{2stored}$ ranged from 1230 kg $CO_2$ (*Ca*) to about 9350 kg $CO_2$ (*Fe*, *Qr*, *Ul*) (Fig. 5D) on 65 years after transplant. Within 20 years after transplanting, *Pn* displayed higher $CO_{2stored}$ than other species.

$CO_2$ sequestration ($CO_{2seq}$, kg tree$^{-1}$ year$^{-1}$) followed a bell-shaped curve when scaled against time after planting in both cities (Fig. 5E, F). Peak $CO_{2seq}$ ranged from 20 kg $CO_2$ year$^{-1}$ (*Ca*) to about 220 kg $CO_2$ year$^{-1}$ (*Fe* and *Ul*). The time after planting for reaching the maximum $CO_2$ sequestration ranged from 1 to 10 (*Pn*) to about 35 years (*Fe*, *Pa*).

### 3.6. Relationship between $CO_2$ assimilation and sequestration

The amount of $CO_2$ sequestered per unit $CO_2$ assimilated ($CO_{2seq}$/ $A_{tree(y)}$) negatively scaled with DBH (P < 0.01; R$^2$ = 0.388 and 0.915 in

Rimini and Krakow, respectively) according to the linear relationship $CO_{2seq}/A_{tree(y)} = b + a*DBH$, where the empiric coefficients a and b differed among species (P < 0.01) (Fig. 6). *Pn* and *Qr* displayed higher intercept than other species in both cities (data not shown). Overall, intercept averaged 0.48 and 0.60 in Rimini and Krakow, respectively.

## 4. Discussion

### 4.1. Species suitability to assimilate, sequester and store $CO_2$

In both cities, *Qr* and *Pn* consistently displayed higher $CO_2$-assimilation per unit leaf area at saturating irradiance ($A_{sat}$) than other species, whereas the lower $A_{sat}$ was found in species belonging to the *Acer* genus. $A_{sat}$ did not scale with stem diameter, indicating that, in unfavourable environments such as cities, growing conditions rather than aging, are primary drivers of photosynthetic rate of fully established trees (Bond, 2000). The annual average $A_{sat}$ was relatively conserved between the climatic areas of the two cities. After normalization using the Normalized Index of Variation [NIV = ($A_{sat}$Rimini – $A_{sat}$Krakow)/($A_{sat}$Rimini + $A_{sat}$Krakow), Tattini et al., 2006], average annual $A_{sat}$ of the co-occurring species *Ah*, *Pn*, and *Qr* differ by only 0.3–7.4 % between Rimini and Krakow.

Conversely, the seasonal trend of $A_{sat}$ underwent larger changes between the cities, seconded by different climatic drivers. In the cold-
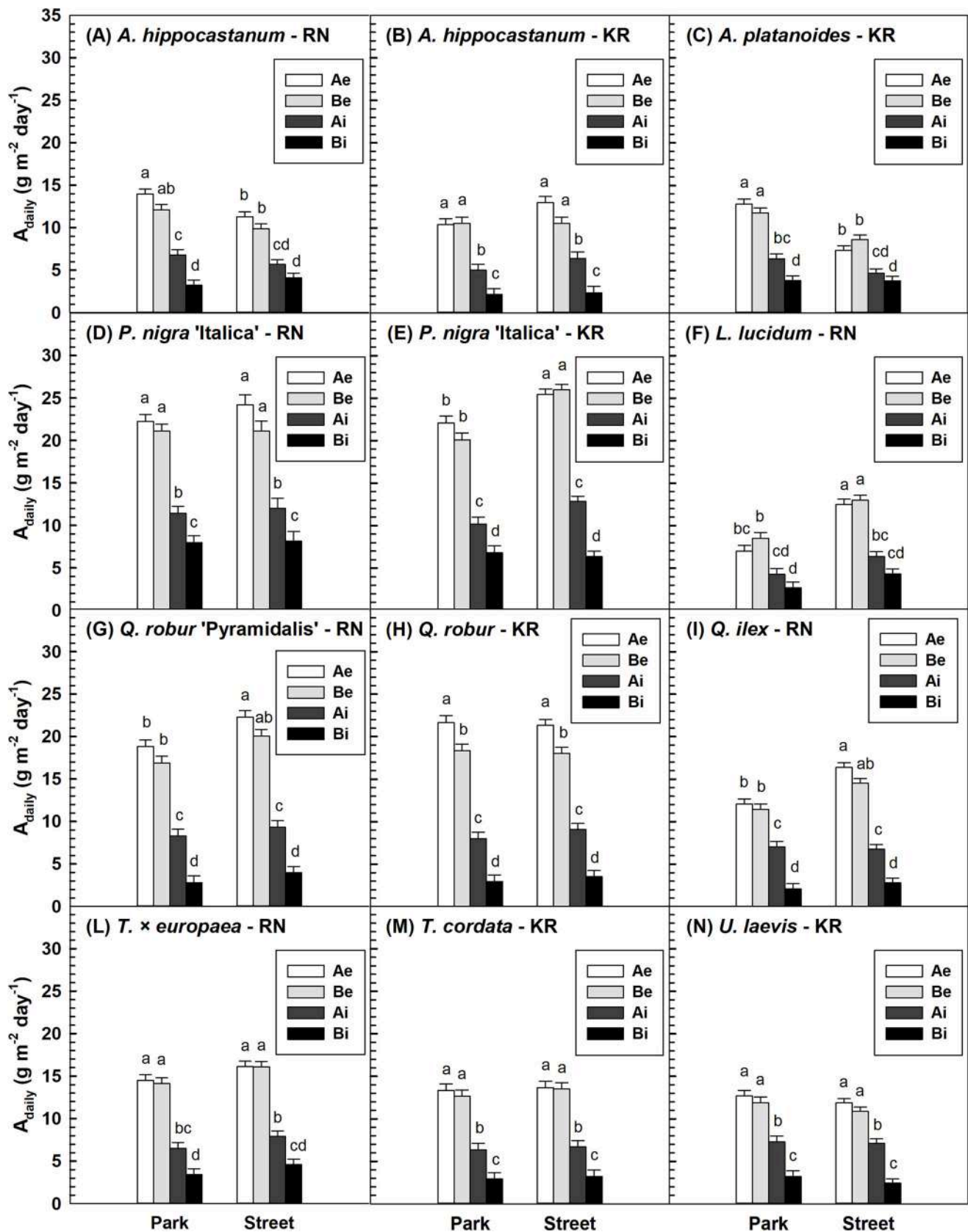
**Fig. 3.** Average ($\pm$ standard deviation) net daily $CO_2$-assimilation per unit leaf area ($A_{daily}$, g $CO_2$ m$^{-2}$ day$^{-1}$) by full sun (Ae and Be) and shaded (Ai and Bi) leaves located in the upper (Ae and Ai) and lower (Be and Bi) canopy layers for different woody species growing in parks and along streets in Rimini (RN: A, D, F, G, I, L) and Krakow (KR: B, C, E, H, M, N). Co-occurring species in the two cities have been paired to increase readability. Different letters indicate significant differences among leaf type and strata within each species, at P < 0.01.
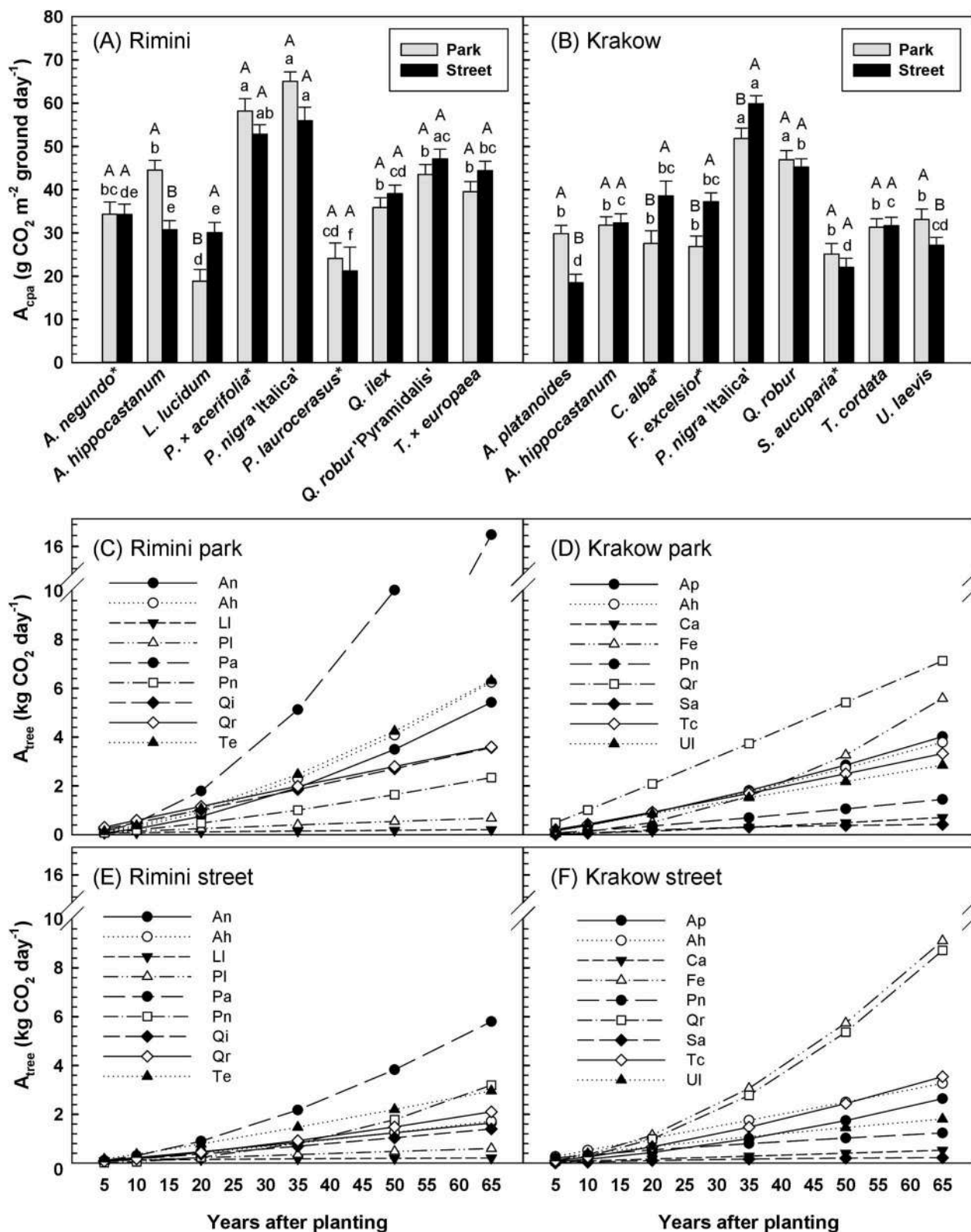
**Fig. 4.** Average ($\pm$ standard deviation) net daily $CO_2$-assimilation per unit crown-projection area estimated using the multilayer model ($A_{cpaML(d)}$, g $CO_2$ m$^{-2}$ ground day$^{-1}$) (A, B) and average net daily $CO_2$-assimilation per tree ($A_{tree}$, g $CO_2$ tree$^{-1}$ day$^{-1}$) (C, D, E, F) calculated over a 65-year lifecycle by different woody species growing in Rimini (A, C, E) and Krakow (B, D, F). In panels A and B, $A_{cpaML(d)}$ values of species marked with + were estimated using the big-leaf model, after correction for the slope of the relationship between $A_{cpaBL(d)}$ and $A_{cpaML(d)}$. Different uppercase letters in panels A and B indicate significant differences between strata at $P < 0.01$, within each species. Different small letters indicate significant differences among species, within each strata, at $P < 0.01$. See table A6 in supplemental materials for full ANOVA table.
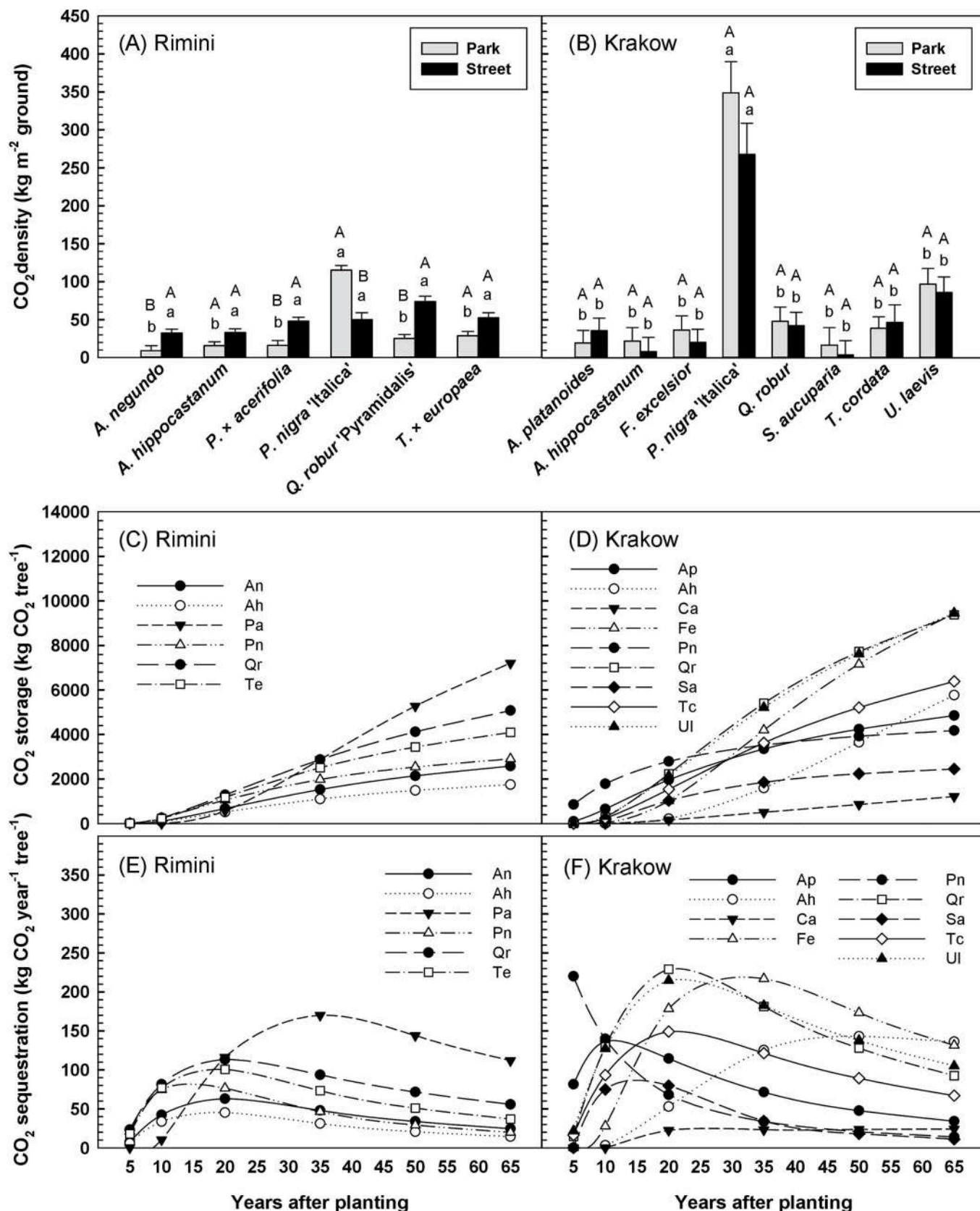
**Fig. 5.** Average ($\pm$ standard deviation) $CO_2$-density (kg $CO_2$ m$^{-2}$ ground) (A, B), and $CO_2$-storage (kg $CO_2$ tree$^{-1}$) (C, D) and $CO_2$-sequestration (kg $CO_2$ tree$^{-1}$ year$^{-1}$) (E, F) calculated over a 65-year lifecycle by different woody species growing in Rimini (A, C, E) and Krakow (B, D, F). Different uppercase letters in panels A and B indicate significant differences between strata at $P < 0.01$, within each species. Different small letters indicate significant differences among species, within each stratum, at $P < 0.01$. See table A4 in supplemental materials for full ANOVA table.
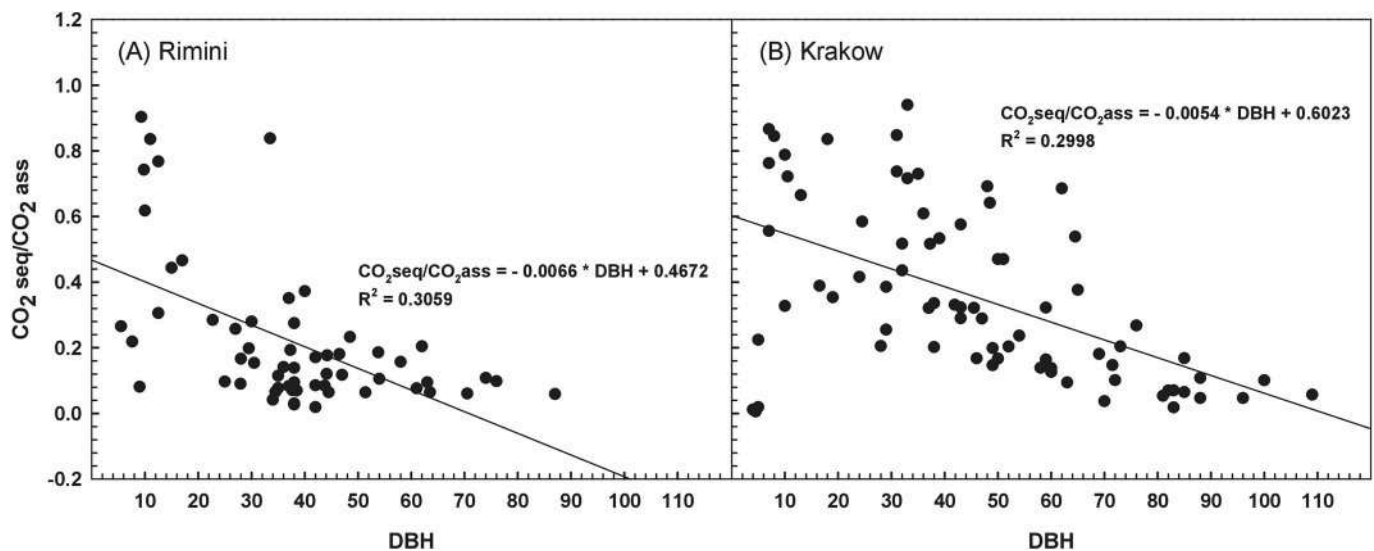
**Fig. 6.** Ratio between $CO_2$-sequestration and $CO_2$-assimilation, both expressed in kg $CO_2$ tree$^{-1}$ year$^{-1}$, as affected by DBH (cm) in Rimini (A) and Krakow (B).

temperate climate of Krakow, low fall temperatures constrained $A_{sat}$ during fall in all species, likely due to non-stomatal limitations (Warren and Adams, 2004), except for the Siberian species Ca. In the hot-summer climate of Rimini, instead, summer drought was key climatic driver which differently influenced $A_{sat}$ according to the species-specific mechanism adopted to cope with drought stress (Kozlowski and Pallardy, 2002). At one side of the spectrum, near-isohydric species, such as *Pa* and *Te*, displayed high $CO_2$-assimilation during spring, but $A_{sat}$ dropped during summer due to high stomatal sensitivity to soil moisture availability and VPD. On the other hand, near-anisohydric species such as oaks maintained stomatal opening during summer, thus sustaining $CO_2$-assimilation despite decreasing water potential. It must be noted that neither strategy could be associated to consistently higher $CO_2$-assimilation by the plant: when leaf values were upscaled to the canopy, both strategies included species capable of both high (*Pa*, *Pn*) and low (*Pl*, *Ll*) average $CO_2$-assimilation per unit crown projection area ($A_{cpaML(d)}$).

In addition to $CO_2$-assimilation per unit leaf area, the amount of leaf area developed on the unit ground area (LAI) is a major driver of $A_{cpaML(d)}$ (Fares et al., 2020). The relationship between LAI and $A_{cpaML(d)}$, however, was shown as parabolic and both low LAI (due to limited light harvesting capacity and photosynthetic area) and excessively high LAI (due to increased self-shading with no proportional increase in photosynthesis) can be detrimental to plant fitness (Pan et al., 2021). Consistently, the species which provided higher $A_{cpaML(d)}$, namely *Pn*, *Qr*, and, in Rimini, *Pa*, were characterized by high photosynthetic rate and LAI in between 3.8 and 4.3 (Rimini) or around 3.5 (Krakow). Conversely, species with low photosynthetic rate, such as *Ah* and *Pl*, failed to achieve high $A_{cpaML(d)}$ although their LAI was very high. Results agree with Pan et al., 2021 who found optimal LAI around 4.5.

$A_{cpaML(d)}$ may be valuable for assessing $CO_2$-assimilation of trees with known canopy size, as well as to assist remote sensing and aerial photography in the estimation of the removal of atmospheric-$CO_2$ by homogeneous canopy covers. More frequently, however, there is interest on $CO_2$-assimilation by individual specimens, which greatly depends on species-specific crown size and canopy growth behaviour over time within the microclimatic conditions of the planting site (Pretzsch et al., 2015). To fill the existing gaps about crown-size allometry of open-growth trees, age-DBH and DBH-crown-radius relationships were developed for 15 woody species. Both relationships well fitted a power function for all species (except *Sa* whose age-DBH relationship better fitted a sigmoid) and the exponent of the DBH-Crown-radius relationship averaged 2/3, conforming to previous research (Rötzer et al., 2020).

Assuming even horizontal distribution of LAI over crown projection area (Rötzer et al., 2019), daily $CO_2$-assimilation by the whole tree ($A_{tree}$) was modelled over an arbitrary 65-year life-cycle. Species which matched high $A_{cpaML(d)}$ and massive canopy spread, such as *Pa* in Rimini and *Qr* in Krakow displayed higher $A_{tree}$ at maturity than other species. At the other end of the spectrum, *Ll* and *Sa*, due to both low $A_{cpaML(d)}$ and crown size, provided lower $A_{tree}$ than other species through their whole life-cycle.

$CO_2$-storage was calculated as function of above-ground volume ($V_{abg}$), which was estimated using a QSM approach based on TLS LiDAR point cloud. Some uncertainty is associated with such measurements, whose accuracy can hardly be tested without destructively harvesting the trees, which was not feasible in this research. Nonetheless, the QSM approach and its modifications, such as AdQSM, have been successfully applied for the estimation of $V_{abg}$ in large-, medium-, and small-sized trees (Raumonen et al., 2013; Fan et al., 2020).

When plotted against DBH, $CO_2$-storage scaled according to a sigmoid (Meinzer et al., 2005) except for *Ca* where the best fit was achieved by linear scaling. Species with higher $A_{tree}$, such as *Pa* in Rimini and *Qr* and *Fe* in Krakow, also displayed higher storage at maturity (Weissert et al., 2017; Fares et al., 2020), although species with high allocation of photosynthates to growth during juvenile phase, such as *Qr* and *Te* in Rimini and *Pn* in both cities, displayed the highest storage among the species investigated during the first 20–30 years after establishment.

Our data underline the need of proper management to extend tree-life span and avoid premature decline (Nowak and Crane, 2002). $CO_2$-storage by a late-mature tree (65 years after transplant) was equivalent to that stored by 382 newly-established (5 years after transplant) individuals of the same species, consistently to Nowak (1994). Our results also agree with size at maturity being a major determinant of $CO_2$-storage per individual tree (Nowak and Crane, 2002), although the use of large trees may not maximize $CO_2$-storage per unit land area, if their $CO_2$-density is low. As an example, if three *P. nigra* 'Italica', a cv. with a narrow canopy and a very high $CO_2$-density, are planted instead of a single *Acer* spp. or *Aesculus*, canopy cover at maturity will be the same, but overall $CO_2$-storage will increase 5-fold.

$CO_2$-sequestration was not constant through the tree life-cycle, rather followed a bell-shaped pattern. The time needed to reach the peak $CO_2$-sequestration and the duration of the peak is likely related to the expected lifespan of each species (Fay and Butler, 2017). These results extend to urban sites the finding obtained in forest environments that net annual carbon sequestration diminishes through time as the forest ages and can become negative during periods of forest decline

(Nowak and Crane, 2002). Peak $CO_2$-sequestration ranged from 20 to 220 kg $CO_2$ per tree per year, consistently with previous estimates (Boukili et al., 2017). Higher sequestration was found in large-sized trees, such as *Pa*, *Qr*, *Fe*, *Ul*, while $CO_2$-sequestration by shrub species was low (Jo and McPherson, 1995; Mori et al., 2016).

### 4.2. $CO_2$-assimilation by park and street trees

The effect of growing environment (i.e. park or street) on $CO_2$-assimilation per unit leaf area ($A_{sat}$) was variable depending on climate, season, and species. In the Cfa climate of Rimini, street trees displayed in general higher $A_{sat}$ than park trees. Even for isohydric species, the summer drop in $A_{sat}$ was lower in street- compared to park-trees, supporting the idea that impermeable pavements may alleviate drought stress during prolonged dry periods by reducing evaporative water losses (Fini et al., 2022). In the cooler Cfb climate of Krakow, the annual average $A_{sat}$ was similar in park and street trees, although $A_{sat}$ was transiently lower in street trees during spring. Such difference may be due to salt damage following extensive application of de-icing salts during winter, since the decline was generally larger in salt-sensitive (e. g. *Sa*, *Tc*) than in salt-tolerant (e.g. *Ulmus*) species (Kratsch et al., 2008).

The effects of strata on $CO_2$-assimilation per unit canopy cover ($A_{cpaML(d)}$) were not consistent across species. Conversely, $CO_2$-assimilation per tree ($A_{tree}$) was lower in street trees, compared to even-aged park trees, for 13 of the 15 species investigated. Such change was mainly driven by declines in CPA, rather than in $A_{cpaML(d)}$, and was more intense in Rimini, where street trees were pruned more severely and often using topping, compared to Krakow (Fig. A.3 in supplemental materials). This suggests that $A_{tree}$ is highly sensitive to pruning method and intensity (Li et al., 2003), particularly for species with broad canopies (Speak and Salbitano, 2023). Consistently, in Rimini, *Ah* ($-71$ %), *Pa* ($-65$ %), and *Qi* ($-65$ %), experienced larger reductions in $A_{tree}$ than species with narrow canopy (e.g. *Pn* $-20$ %) when grown along streets, compared to parks. Conversely, severe pruning increased $CO_2$-density in street trees of Rimini, because pruning induced larger reductions in crown-projection-area than in $CO_2$-storage.

### 4.3. Relationship between $CO_2$-assimilation and sequestration

This research upscaled measured leaf gas exchange per unit leaf area data to the whole tree using either a big-leaf and a multilayer approach, to compare it with $CO_2$-sequestration estimated from annual woody biomass increment. Results highlighted that the contribution of woody species in lowering atmospheric $CO_2$ may be underestimated if $CO_2$-sequestration, rather than net $CO_2$-assimilation, is considered as reference parameter. Similar findings were obtained when $CO_2$ sequestration estimated by allometric curves was compared to Net Primary Productivity measured by Eddy-Covariance (Velasco et al., 2016). The amount of freshly-assimilated-$CO_2$ allocated to woody biomass growth was inversely related to stem diameter and ranged between 48 and 60 % for newly established trees to about 10 % for late mature trees, consistently with previous estimates (Velasco et al., 2016).

Leaf, but not root, respiration was considered in this research which is acknowledged as a possible limitation of this research. This was due to technical challenges in partitioning in situ root autotrophic respiration (which depends on species-specific root traits, such as specific-root-length) from heterotrophic respiration (which is mostly driven by soil temperature and can occur at high rates even in unrooted soils) (Loveys et al., 2003; Black et al., 2016; Ferlian et al., 2017; Borden et al., 2021). Previous research conducted using C-isotope-discrimination revealed that root autotrophic respiration accounted for 2.1–11.5 % of freshly assimilated carbon (Pumpanen et al., 2009; Qubaja et al., 2020), thus it may only partially explain the differences between $CO_2$-assimilation and sequestration.

Several alternative fates can occur to freshly-assimilated $CO_2$ and can contribute to trap $CO_2$ as organic compounds without directly affecting

tree volume change and $CO_2$-sequestration: 1) allocation to secondary metabolites, such as phytoanticipins and phytoalexins accumulated in the xylem (Morris et al., 2019); 2- allocation to ephemeral above-ground organs, whose contribution to long-term $CO_2$ abatement may depend on municipal management strategies (Nowak et al., 2002); 3- allocation to fine roots and mycorrhizal biomass, which can be stored as soil-C pool (Pumpanen et al., 2009; Mathew et al., 2020); 4- build-up of starch, stored as reserve in tree parenchyma. A full characterization of the allocation of freshly-assimilated $CO_2$ was, however, beyond the aims of this research, which was instead aimed at evaluating the potential of different species for photosynthetic $CO_2$ uptake.

A second limitation is that leaf gas exchange was measured in sunny days, and little information was collected about photosynthetic rates under the sub-saturating light availability set by cloud-cover. Future research aimed at calculating photosynthetic traits through the fitting of representative light response (A/PPFD) curves for sun and shaded leaves of the different species may be crucial for increasing the accuracy of net $CO_2$ uptake estimates during cloudy days.

### 4.4. Effect of big-leaf and multilayer upscaling method on canopy photosynthesis

Two distinct models were used to upscale $CO_2$-assimilation per unit leaf area to canopy photosynthesis: a big-leaf and a multilayer model. Although photosynthesis data were highly consistent when leaves experiencing similar irradiance were compared (see $A_{sat}$, $A_{daily,ae}$ and $A_{daily,be}$ in Figs. 2 and 3), the big-leaf under-estimated $CO_2$-assimilation compared to the sun-shade, and the under-estimation was lower at higher latitudes ($-31$ % in Rimini; $-6.5$ % in Krakow) and was species-specific. Such results conformed with previous research conducted in forest environment (Sprintsin et al., 2012), although the accuracy of big-leaf was higher than expected in Krakow.

Different reasons may explain the different accuracy of the big-leaf, compared to the multilayer model, in the two cities. Firstly, decreasing light availability for shaded leaves at increasing latitudes was reported because of declines in both direct and diffuse radiation (Sprintsin et al., 2012; see also Table A.1 in supplemental materials). In such conditions, productivity of shaded leaves can be lower than at southern latitudes, resulting in increased consistency between the two models. Secondly, decreasing accuracy of the Beer's law in describing radiation distribution at increasing LAI has been proposed as a possible explanation for big-leaf underestimations (Luo et al., 2018). Consistently, in this research, LAI was on average 17 % higher in Rimini than in Krakow. Thirdly, discrepancies between models have been reported to increase with canopy clumping (Sprintsin et al., 2012). Although we did not measure clumping directly, calculated clumping of common species was slightly higher in street trees of Rimini compared to Krakow, likely due to pruning history. Finally, the ability of the different species to tolerate self-shading through morphological, structural, and physiological adjustments occurring at the leaf level may contribute explaining the differences in accuracy between the two models (Fini et al., 2016; Poorter et al., 2019). However, shade acclimation seems more explanatory of differences between models observed among species within each city than of differences between cities. At 90 % reduction of above canopy irradiance, as it may be typically experienced by shaded leaves in the lower canopy, carbon gain of strictly sun-requiring species such as *Qr* was about 82 % lower compared to full sun leaves in both cities. Conversely, at the same light availability, the reduction in photosynthetic rate of shaded leaves of shade-tolerant species such as *Ll* and *Ap* was only 62–68 %, compared to full-sun leaves.

## 5. Conclusions

At the individual tree scale, we showed that large-sized species with a broad canopy at maturity and a high net photosynthetic rate per unit crown projection area ($A_{cpa}$), such as *Pa* and *Qr*, were more effective to

assimilate $CO_2$. At the whole-city scale, overall $CO_2$ assimilation can be maximised for a given canopy cover using species with high $A_{cpa}$, although care must be paid to avoid monospecific plantations which can be highly susceptible to specialist pest and pathogen outbreak. A mixture of species with large canopies, such as *Pa*, *Qr*, and species with narrow canopy planted at higher densities (e.g. *Pn* 'Italica', *Qr* 'Fastigiata') may thus be recommended for maximizing $CO_2$ uptake while maintaining biodiversity. Our results support the notion that shaded leaves shall be considered for an accurate estimation of $A_{cpa}$, since the big-leaf model underestimated $A_{cpa}$ with larger under-estimations at lower latitudes, on plants with high LAI and clumping, and on shade-tolerant species. Future research is needed for accurate parametrization of photosynthetic properties of shaded leaves, which have been neglected by leaf gas exchange research so far. No evidence of chronic physiological stress was detected on street- compared to park-trees, although whole-plant $CO_2$-assimilation by street trees can be constrained if severe pruning chronically reduces canopy size.

The species which displayed the higher whole-tree $CO_2$-assimilation also showed higher $CO_2$-storage and -sequestration. Our research, however, highlights the importance of including photosynthetic traits in the estimation of atmospheric-$CO_2$ removal, to avoid underestimation which may occur if $CO_2$-sequestration is considered as reference parameter. The amount of freshly-assimilated $CO_2$ sequestered as new woody biomass ranged from 48 % to 60 % in young trees and decreased with tree age, underlying that alternative metabolic fates of assimilated-$CO_2$ other than woody biomass production may thus play a role in lowering atmospheric $CO_2$, particularly for old trees. $CO_2$-assimilation data collected in situ as well as allometric equations specifically developed for trees growing in urban sites may provide direct guidance to city planners as well as may provide a tool for researchers to calibrate and validate process-based models.

## Funding

## CRediT authorship contribution statement

**Alessio Fini:** Conceptualization, Formal analysis, Funding acquisition, Investigation, Methodology, Writing – original draft. **Irene Vigevani:** Data curation, Investigation, Writing – original draft, Visualization. **Denise Corsini:** Data curation, Investigation, Writing – review & editing. **Piotr Węzyk:** Investigation, Methodology, Writing – original draft. **Katarzyna Bajorek-Zydroń:** Data curation, Investigation. **Osvaldo Failla:** Project administration, Writing – review & editing. **Edoardo Cagnolati:** Conceptualization, Resources, Writing – review & editing. **Lukasz Mielczarek:** Conceptualization, Resources, Writing – review & editing. **Sebastien Comin:** Data curation. **Marco Gibin:** Investigation. **Alice Pasquinelli:** Project administration, Visualization. **Francesco Ferrini:** Supervision, Resources, Writing – review & editing. **Paolo Viskanic:** Conceptualization, Funding acquisition, Project administration, Supervision, Visualization.

## Declaration of competing interest

The authors declare that they have no known competing financial interests or personal relationships that could have appeared to influence the work reported in this paper.

## Data availability

Data will be made available on request.

## Appendix A. Supplementary data

Supplementary data to this article can be found online at https://doi.org/10.1016/j.scitotenv.2023.166198.

## References

Aguaron, E., McPherson, E.G., 2012. Comparison of methods for estimating carbon dioxide storage by Sacramento's urban forest. In: Lal, R., Augustin, B. (Eds.), Carbon Sequestration in Urban Ecosystems. Springer, Dordrecht, pp. 43–71.

Allen, R.G., Pereira, L.S., Raes, D., Smith, M., 1998. Crop evapotranspiration - guidelines for computing crop water requirements. In: FAO Irrigation and Drainage Paper, 56. Rome.

Black, C.K., Davis, S.C., Hudiburg, T.W., Bernacchi, C.J., DeLucia, E.H., 2016. Elevated $CO_2$ and temperature increase soil C losses from a soybean–maize ecosystem. Glob. Chang. Biol. 23, 435–445.

Bonan, G.B., Patton, E.G., Finnigan, J.J., Baldocchi, D.D., 2021. Moving beyond the incorrect but useful paradigm: reevaluating big-leaf and multilayer plant canopies to model biosphere-atmosphere fluxes – a review. Agric. For. Meteorol. 306, 108435.

Bond, B.J., 2000. Age-related changes in photosynthesis of woody plants. Trends Plant Sci. 5, 349–353.

Boni Vicari, M., Pisek, J., Disney, M., 2019. New estimates of leaf angle distribution from terrestrial LiDAR: comparison with measured and modelled estimates from nine broadleaf tree species. Agric. For. Meteorol. 264, 322–333.

Borden, K.A., Mafa-Attoye, T.G., Dunfield, K.E., Thevathasan, N.V., Gordon, A.M., Isaac, M.E., 2021. Root functional trait and soil microbial coordination: implications for soil respiration in riparian agroecosystems. Front. Plant Sci. 12, 681113.

Boukili, V.K.S., Bebber, D.P., Mortimer, T., Venicx, G., Lefcourt, D., Chandler, M., Eisenberg, C., 2017. Assessing the performance of urban forest carbon sequestration models using direct measurements of tree growth. Urban For. Urban Green 24, 212–221.

Brunetti, C., Tattini, M., Guidi, L., Velikova, V., Ferrini, F., Fini, A., 2019. An integrated overview of physiological and biochemical responses of *Celtis australis* to drought stress. Urban For. Urban Green 46, 126480.

Campbell, G.S., 1986. Extinction coefficients for radiation in plant canopies calculated using an ellipsoidal inclination angle distribution. Agric. For. Meteorol. 36, 317–321.

Chianucci, F., Pisek, J., Raabe, K., Marchino, L., Ferrara, C., Corona, P., 2018. A dataset of leaf inclination angles for temperate and boreal broadleaf woody species. Ann. For. Sci. 75, 50.

De Mattos, E.M., Binkley, D., Campoe, O.C., Alvares, C.A., Stape, J.L., 2020. Variation in canopy structure, leaf area, light interception and light use efficiency among *Eucalytus* clones. Forest Ecol. Manag. 463, 118038.

De Pury, D.G.G., Farquhar, G.D., 1997. Simple scaling of photosynthesis from leaves to canopies without the errors of big-leaf models. Plant Cell Environ. 20, 537–557.

Fan, G., Nan, L., Dong, Y., Su, X., Chen, F., 2020. AdQSM: a new method for estimating above-ground biomass from TLS point clouds. Remote Sens. 12, 3089.

Fares, S., Conte, A., Alivernini, A., Chianucci, F., Grotti, M., Zappitelli, I., Petrella, F., Corona, P., 2020. Testing removal of carbon dioxide, ozone, and atmospheric particles by urban parks in Italy. Environ. Sci. Technol. 54, 14910–14922.

Farquhar, G.D., von Caemmerer, S., Berry, J.A.A., 1980. Biochemical model of photosynthetic $CO_2$ assimilation in leaves of C3 species. Planta 149, 78–90.

Fay, N., Butler, J., 2017. Management and conservation of ancient and other veteran trees. In: Ferrini, F., Konijnendijk, C., Fini, A. (Eds.), Routledge Handbook of Urban Forestry. Routledge, London, pp. 500–514.

Ferlian, O., Wirth, C., Eisenhauer, N., 2017. Leaf and root C-to-N ratios are poor predictors of soil microbial biomass C and respiration across 32 tree species. Pedobiologia 65, 16–23.

Fini, A., Guidi, L., Giordano, C., Baratto, M.C., Ferrini, F., Brunetti, C., Calamai, L., Tattini, M., 2014. Salinity stress constrains photosynthesis in *Fraxinus ornus* more when growing in partial shading than in full sunlight: consequences for the antioxidant defence system. Ann. Bot. 114, 525–538.

Fini, A., Frangi, P., Faoro, M., Piatti, R., Amoroso, G., Ferrini, F., 2015. Effects of different pruning methods on an urban tree species: a four-year-experiment scaling down from the whole tree to the chloroplasts. Urban For. Urban Green 14, 664–674.

Fini, A., Loreto, F., Tattini, M., Giordano, C., Ferrini, F., Brunetti, C., Centritto, M., 2016. Mesophyll conductance plays a central role in leaf functioning of Oleaceae species exposed to contrasting sunlight irradiance. Physiol. Plant. 157, 54–68.

Fini, A., Frangi, P., Comin, S., Vigevani, I., Rettori, A., Brunetti, C., Baesso-Moura, B., Ferrini, F., 2022. Effects of pavements on established urban trees: growth, physiology, ecosystem services and disservices. Landsc. Urban Plan. 226, 104501.

Grimm, B.G., Faeth, S.H., Golubiewski, N.E., Redman, C.L., Wu, J., Bai, X., Briggs, J.M., 2008. Global change and the ecology of cities. Science 319, 756–760.

Hagemeier, M., Leuschner, C., 2019. Functional crown architecture of five temperate broadleaf tree species: vertical gradients in leaf morphology, leaf angle, and leaf area density. Forests 10, 265.

Jo, H.-K., McPherson, E.G., 1995. Carbon storage and flux in urban residential greenspace. J. Environ. Manag. 45, 109–133.

Kannenberg, S.A., Guo, J.S., Novick, K.A., Anderegg, W.R.L., Feng, X., Kennedy, D., Konings, A.G., Martínez-Vilalta, J., Matheny, A.M., 2022. Opportunities, challenges and pitfalls in characterizing plant water-use strategies. Funct. Ecol. 36, 24–37.

Kozlowski, T.T., Pallardy, S.G., 2002. Acclimation and adaptive responses of woody plants to environmental stresses. Bot. Rev. 68, 270–334.

Kratsch, H., Olsen, S., Rupp, L., Cardon, G., Heflebower, R., 2008. Soil Salinity and Ornamental Plant Selection. Utah State University Cooperative Extension, 8 pp.

Leblanc, S.G., Chen, J.M., 2001. A practical scheme for correcting multiple scattering effects on optical LAI measurements. Agric. For. Meteorol. 110, 125–139.

Li, K.T., Lakso, A.N., Piccioni, R., Robinson, T., 2003. Summer pruning reduces whole-canopy carbon fixation and transpiration in apple trees. J. Hortic. Sci. Biotechnol. 78, 749–754.

Loveys, B.R., Atkinson, L.J., Sherlock, D.J., Roberts, R.L., Fitter, A.H., Atkin, O.K., 2003. Thermal acclimation of leaf and root respiration: an investigation comparing inherently fast- and slow-growing species. Glob. Chang. Biol. 9, 895–910.

Luo, X., Chen, J.M., Liu, J., Black, T.A., Croft, H., Staebler, R., He, L., Altaf Arain, M., Chen, B., Mo, G., Gonsamo, A., McCaughey, H., 2018. Comparison of big-leaf, two-big-leaf, and two-leaf upscaling schemes for evapotranspiration estimation using coupled carbon-water modeling. J. Geophys. Res. Biogeosci. 123, 207–225.

Magarik, Y.A.S., Roman, L.A., Henning, J.G., 2020. How should we measure the DBH of multi-stemmed trees? Urban For. Urban Green 47, 126481.

Mathew, I., Shimelis, H., Mutema, M., Minasny, B., Clapot, V., 2020. Crops for increasing soil organic carbon stocks – a global meta-analysis. Geoderma 367, 114230.

Meinzer, F.C., Bond, B.J., Warren, J.M., Woodruff, D.R., 2005. Does water transport scale universally with tree size? Funct. Ecol. 19, 558–565.

Mori, J., Fini, A., Burchi, G., Ferrini, F., 2016. Carbon uptake and air pollution mitigation of different evergreen shrub species. Arboric. Urban For. 42, 329–334.

Morris, H., Hietala, A.M., Jansen, S., Ribera, J., Rosner, S., Salmeida, K.A., Schwarze, F. W.M.R., 2019. Using the CODIT model to explain secondary metabolites of xylem in defence systems of temperate trees against decay fungi. Ann. Bot. 125, 701–720.

Norman, J.M., Jarvis, P.J., 1975. Photosynthesis in Sitka sprouce (*Picea sitchensis* (bong.) Carr.) V. radiation penetration theory and a test case. J. Appl. Ecol. 12, 839–878.

Nowak, D.J., 1994. Atmospheric carbon dioxide reduction by Chicago's urban forest. In: McPherson, E.G., Nowak, D.J., Rowntree, R.A. (Eds.), Chicago's Urban Forest Ecosystem: Results of the Chicago Urban Forest Climate Project. USDA Forest Service General Technical Report NE-186, Radnor, PA, pp. 83–94.

Nowak, D.J., Crane, D.E., 2002. Carbon storage and sequestration by urban trees in the USA. Environ. Pollut. 116, 381–389.

Nowak, D.J., Stevens, J.C., Sisinni, S.M., Luley, C.J., 2002. Effects of urban tree management and species selection on atmospheric carbon dioxide. J. Arboric. 28, 113–122.

Nowak, D., Greenfield, E., Hoehn, R., Lapoint, E., 2013. Carbon storage and sequestration by trees in urban and community areas of the United States. Environ. Pollut. 178, 229–230.

Pan, N., Wang, S., Wei, F., Shen, M., Fu, B., 2021. Inconsistent changes in NPP and LAI determined from the parabolic LAI versus NPP relationship. Ecol. Indic. 131, 108134.

Picard, N., Saint-André, L., Henry, M., 2012. Manual for Building Tree Volume and Biomass Allometric Equations: From Field Measurement to Prediction. Food and Agricultural Organization of the United Nations, Rome, and Centre de Coopération Internationale en Recherche Agronomique Pour le Développement, Montpellier, 215 pp.

Poorter, H., Niinements, U., Ntagkas, N., Siebenkas, A., Maenpaa, M., Matsubara, S., Pons, T.L., 2019. A meta-analysis of plant responses to light intensity for 70 traits ranging from molecules to whole plant performance. New Phytol. 223, 1073–1105.

Pretzsch, H., Biber, P., Uhl, E., Dahlhausen, J., Rötzer, T., Caldentey, J., Koike, T., van Con, T., Chavanne, A., Seifert, T., du Toit, B., Farnden, C., Pauleit, S., 2015. Crown size and growing requirement of common tree species in urban centres, parks, and forests. Urban For. Urban Green 14, 466–479.

Pumpanen, J.S., Heinonsalo, J., Rasilo, T., Hurme, K.R., Ilvesniemi, H., 2009. Carbon balance and allocation of assimilated $CO_2$ in scots pine, Norway spruce, and silver birch seedlings determined with gas exchange measurements and 14C pulse labelling. Trees 23, 611–621.

Qubaja, R., Tatarinov, F., Rotenberg, E., Yakir, D., 2020. Partitioning of canopy and soil $CO_2$ fluxes in a pine forest at the dry timberline across a 13-year observation period. Biogeosciences 17, 699–714.

Raumonen, P., Kaasalainen, M., Åkerblom, M., Kaasalainen, S., Kaartinen, H., Vastaranta, M., Holopainen, M., Disney, M., Lewis, P., 2013. Fast automatic precision tree models from terrestrial laser scanner data. Remote Sens. 5, 491–520.

Rötzer, T., Rahman, M.A., Moser-Reischl, A., Pauleit, S., Pretzsch, H., 2019. Process based simulation of tree growth and ecosystem services of urban trees under present and future climatic conditions. Sci. Total Environ. 676, 651–664.

Rötzer, T., Moser-Reischl, A., Rahman, M.A., Grote, R., Pauleit, S., Pretzsch, H., 2020. Modelling urban tree growth and ecosystem services: review and perspectives. In: Cánovas, F.M., Lüttge, U., Risueño, M.C., Pretzsch, H. (Eds.), Progress in Botany, 82, pp. 450–464.

Savi, T., Bertuzzi, S., Branca, S., Tretiach, M., Nardini, A., 2015. Drought-induced xylem cavitation and hydraulic deterioration: risk factors for urban trees under climate change? New Phytol. 205, 1106–1116.

Sharma, Y., Singh, H., Singh, S., 2018. Effect of light interception and penetration at different levels of fruit tree canopy on quality of peach. Curr. Sci. India 115, 1562–1566.

Speak, A.F., Salbitano, F., 2023. The impact of pruning and mortality on urban tree canopy volume. Urban For. Urban Green 79, 127810.

Sprintsin, M., Chen, J.M., Desai, A., Gough, C.M., 2012. Evaluation of leaf-to-canopy upscaling methodologies against carbon flux data in North America. J. Geophys. Res. 117, G01023.

Tattini, M., Remorini, D., Pinelli, P., Agati, G., Saracini, E., Traversi, M., Massai, R., 2006. Morpho-anatomical, physiological and biochemical adjustments in response to root zone salinity stress and high solar radiation in two Mediterranean evergreen shrubs, *Myrtus communis* and *Pistacia lentiscus*. New Phytol. 170, 779–794.

Velasco, E., Roth, M., Norford, L., Molina, L.T., 2016. Does urban vegetation enhance carbon sequestration? Landsc. Urban Plan. 148, 99–107.

Warren, C.R., Adams, M.A., 2004. Evergreen trees do not maximize instantaneous photosynthesis. Trends Plant Sci. 9, 270–274.

Weissert, L.F., Salmond, J.A., Schwendenmann, L., 2017. Photosynthetic $CO_2$ uptake and carbon sequestration potential of deciduous and evergreen tree species in an urban environment. Urban Ecosyst. 20, 663–674.

Wilcox, M., 2000. Tree privet (*Ligustrum lucidum*)–a controversial plant. Auckland Bot. Soc. J. 55, 72–74.

Yan, G., Hu, R., Luo, J., Weiss, M., Jiang, H., Mu, X., Xie, D., Zhang, W., 2019. Review of indirect optical measurements of leaf area index: recent advances, challenges, and perspectives. Agric. For. Meteorol. 265, 390–411.

Yoon, T.K., Park, C.W., Lee, S.J., Ko, S., Kim, K.N., Son, Y., Lee, K.H., Oh, S., Lee, W.K., Son, Y., 2013. Allometric equations for estimating the aboveground volume of five common urban street tree species in Daegu, Korea. Urban For. Urban Green 12, 344–349.

Zanne, A.E., Lopez-Gonzalez, G., Coomes, D.A., Ilic, J., Jansen, S., Lewis, S.L., Miller, R. B., Swenson, N.G., Wiemann, M.C., Chave, J., 2009. Global Wood Density Database. Dryad. http://hdl.handle.net/10255/dryad.235.

Contents lists available at ScienceDirect

# Science of the Total Environment

journal homepage: www.elsevier.com/locate/scitotenv

Corrigendum

# Corrigendum to "CO2-assimilation, sequestration, and storage by urban woody species growing in parks and along streets in two climatic zones" [Science of the Total Environment (2023) article number 166198]

Alessio Fini [a,*], Irene Vigevani [a,b,c], Denise Corsini [a,b], Piotr Wężyk [d,e],
Katarzyna Bajorek-Zydroń [d], Osvaldo Failla [a], Edoardo Cagnolati [f], Lukasz Mielczarek [g],
Sebastien Comin [a], Marco Gibin [a], Alice Pasquinelli [h], Francesco Ferrini [b,i], Paolo Viskanic [h]

[a] Department of Agricultural and Environmental Sciences—Production, Landscape, Agroenergy, University of Milan, Milan 20133, Italy
[b] Department of Agriculture, Food, Environment and Forestry, University of Florence, Florence 50144, Italy
[c] University School for Advanced Studies Pavia, Pavia 27100, Italy
[d] ProGea 4D sp. z o o, ul. Pachońskiego 9, Kraków 31-223, Poland
[e] University of Agriculture in Krakow, Krakow 31-120, Poland
[f] Anthea S.r.l, Via della Lontra 30, Rimini 47923, Italy
[g] Zarząd Zieleni Miejskiej w Krakowie (ZZM), ul. Reymonta 20, Kraków 30-059, Poland
[h] R3 GIS S.r.l. NOI Techpark, D1, Via Ipazia 2, Bolzano 39100, Italy
[i] National Biodiversity Future Center (www.nbfc.it), Italy

The authors regret that the printed version of the above article contained a number of errors in Table 2. The errors were due to the use of comma, instead of dot, as decimal separator in the last three columns from the right side of the table (those reporting the allometric coefficients for $V_{abg}$ estimation). Commas were then deleted during printing, thus increasing the coefficients B by three order of magnitude (e.g. 1.653 to 1653). We feel that keeping such values not corrected may result in the non-applicability of the equations proposed by this publication. The correct and final version of Table 2 follows. The authors would like to apologise for any inconvenience caused.

**Table 2**

Wellness of fit ($R^2$) and empirical coefficients (a and b) to fit the allometric relationships to estimate: 1- Stem diameter at breast height (tree species) or at the lowest fork (shrub species) (DBH, cm) from time after transplant (Age, years); 2- crown radius (Cr, m) from DBH (cm) in park and street trees, and 3- above-ground volume ($V_{abg}$, m$^3$) from DBH (cm) in a Cfa (Rimini) and Cfb (Krakow) climate. $V_{abg}$ was not determined (N.D.) on evergreen species. DT = deciduous tree; DS = deciduous shrub; ET = evergreen tree; ES = evergreen shrub.

| Species | City | DBH = b * Age$^a$ or DBH = e$^{((b+(a/age))}$ (*S. aucuparia*) | | | Cr = b * DBH$^a$ (park trees) | | | Cr = b * DBH$^a$ (street trees) | | | $V_{abg}$ = e$^{((b+(a/DBH))}$ or $V_{abg}$ = b + a * DBH (*C. alba*) | | |
|---|---|---|---|---|---|---|---|---|---|---|---|---|---|
| | | a | b | R2 | a | b | R2 | a | b | R2 | a | b | R2 |
| *A. negundo* (DT) | Rimini | 0.9240 | 1.1139 | 0.883 | 0.9056 | 0.1955 | 0.756 | 0.5763 | 0.3973 | 0.634 | −35.77 | 1.653 | 0.884 |
| *A. platanoides* (DT) | Krakow | 0.7990 | 1.8168 | 0.873 | 0.7491 | 0.3184 | 0.871 | 0.7491 | 0.3184 | 0.871 | −29.49 | 1.966 | 0.947 |
| *A. hippocastanum* (DT) | Rimini | 0.9996 | 0.9590 | 0.947 | 0.8098 | 0.2356 | 0.789 | 0.6053 | 0.3366 | 0.873 | −33.65 | 0.942 | 0.831 |
| *A. hippocastanum* (DT) | Krakow | 0.9187 | 1.5088 | 0.896 | 0.6772 | 0.3467 | 0.947 | 0.5007 | 0.6290 | 0.376 | −117.06 | 3.269 | 0.930 |
| *C. alba* (DS) | Krakow | 1.0627 | 0.2522 | 0.847 | 0.6368 | 0.4052 | 0.903 | 0.4666 | 0.4981 | 0.613 | 0.046 | −0.170 | 0.994 |
| *F. excelsior* (DT) | Krakow | 1.1137 | 0.7448 | 0.942 | 0.9197 | 0.1482 | 0.913 | 0.7910 | 0.2817 | 0.746 | −63.73 | 2.794 | 0.639 |
| *L. lucidum* (ET) | Rimini | 0.4507 | 3.5630 | 0.416 | 0.5777 | 0.3006 | 0.289 | 0.3381 | 0.5105 | 0.306 | N.D. | N.D. | N.D. |
| *P. x acerifolia* (DT) | Rimini | 1.1462 | 0.6502 | 0.858 | 0.8212 | 0.2654 | 0.905 | 0.6915 | 0.2910 | 0.863 | −69.18 | 2.603 | 0.918 |
| *P. nigra* 'Italica' (DT) | Rimini | 1.0084 | 1.2849 | 0.897 | 0.6756 | 0.1662 | 0.854 | 1.1093 | 0.0303 | 0.778 | −38.30 | 1.699 | 0.936 |
| *P. nigra* 'Italica' (DT) | Krakow | 0.7047 | 4.2950 | 0.777 | 0.8464 | 0.0719 | 0.572 | 0.4997 | 0.2839 | 0.466 | −25.28 | 1.930 | 0.957 |
| *P. laurocerasus* (ES) | Rimini | 0.6141 | 2.2546 | 0.468 | 0.6978 | 0.2830 | 0.340 | 0.6978 | 0.2830 | 0.340 | N.D. | N.D. | N.D. |
| *Q. ilex* (ET) | Rimini | 0.6628 | 2.9073 | 0.781 | 0.8016 | 0.2604 | 0.907 | 0.8592 | 0.1251 | 0.826 | N.D. | N.D. | N.D. |
| *Q. robur* 'Pyramidalis' (DT) | Rimini | 0.7582 | 2.1014 | 0.736 | 0.6342 | 0.4305 | 0.630 | 0.8792 | 0.1213 | 0.775 | −47.23 | 2.266 | 0.920 |
| *Q. robur* (DT) | Krakow | 0.9786 | 1.2701 | 0.920 | 0.5339 | 0.6912 | 0.734 | 0.9455 | 0.1313 | 0.940 | −50.00 | 2.629 | 0.715 |
| *S. aucuparia* (DT) | Krakow | −14.56 | 3.6582 | 0.745 | 0.7792 | 0.1579 | 0.872 | 0.7579 | 0.1323 | 0.687 | −40.90 | 1.829 | 0.950 |
| *T. cordata* (DT) | Krakow | 0.8777 | 1.6516 | 0.767 | 0.6201 | 0.4390 | 0.825 | 0.8091 | 0.2049 | 0.921 | −50.51 | 2.649 | 0.950 |
| *T. x europaea* (DT) | Rimini | 0.9031 | 1.5039 | 0.887 | 0.8404 | 0.2128 | 0.898 | 0.6275 | 0.3348 | 0.839 | −42.73 | 1.941 | 0.955 |
| *U. laevis* (DT) | Krakow | 0.8536 | 1.7177 | 0.908 | 0.5970 | 0.4513 | 0.477 | 0.4866 | 0.6239 | 0.772 | −51.77 | 2.845 | 0.893 |